

NASA Contractor Report 187475

ICASE Report No. 90-81

ICASE

THE INVISCID STABILITY OF SUPERSONIC FLOW PAST HEATED OR COOLED AXISYMMETRIC BODIES

Stephen J. Shaw

Peter W. Duck

Contract No. NAS1-18605

November 1990

Institute for Computer Applications in Science and Engineering

NASA Langley Research Center

Hampton, Virginia 23665-5225

Operated by the Universities Space Research Association



National Aeronautics and
Space Administration

Langley Research Center

Hampton, Virginia 23665-5225

(NASA-CR-187475) THE INVISCID STABILITY OF
SUPERSONIC FLOW PAST HEATED OR COOLED
AXISYMMETRIC BODIES Final Report (ICASE)

54 p

CSCL 01A

N91-14307

Unclass

G3/02 0320477

THE INVISCID STABILITY OF SUPERSONIC FLOW PAST HEATED OR COOLED AXISYMMETRIC BODIES

Stephen J. Shaw

and

Peter W. Duck¹

Department of Mathematics

University of Manchester

ENGLAND

ABSTRACT

The inviscid, linear, non-axisymmetric, temporal stability of the boundary layer associated with the supersonic flow past axisymmetric bodies (with particular emphasis on long thin, straight circular cylinders), subject to heated or cooled wall conditions is investigated. The eigenvalue problem is computed in some detail for a particular Mach number of 3.8, revealing that the effect of curvature and the choice of wall conditions both have a significant effect on the stability of the flow.

Both the asymptotic, large azimuthal wavenumber solution and the asymptotic, far downstream solution are obtained for the stability analysis and compared with numerical results. Additionally, asymptotic analyses valid for large radii of curvature with cooled/heated wall conditions, are presented. We find, in general, important differences exist between the wall temperature conditions imposed in this paper and the adiabatic wall conditions considered previously.

¹Research was supported by the National Aeronautics and Space Administration under NASA Contract No. NAS1-18605 while the author was in residence at the Institute for Computer Applications in Science and Engineering (ICASE), NASA Langley Research Center, Hampton, VA 23665.

§1. Introduction and Motivation

The recent resurgence of interest in high speed flight vehicles has rekindled interest in supersonic and hypersonic flows. One important area of aerodynamic study is that of boundary-layer stability and the possible transition to turbulence. Since turbulent flows result in considerably greater skin frictions and heat transfer coefficients than do laminar flows, any method by which a boundary layer may be stabilized is worthy of investigation.

Generally it is found in the case of supersonic boundary-layer flows that inviscid disturbances are more important (i.e. more unstable) than viscous disturbances. (Here, we characterise inviscid disturbances as being those with wavelengths comparable to the boundary-layer thickness, whilst viscous disturbances possess much longer wavelengths). This is in contrast to the situation encountered for many incompressible boundary-layer flows where viscous instabilities are generally dominant. The first authors to give any form of rigorous mathematical account of the stability of compressible boundary layers were Lees and Lin (1). Making use of a rational asymptotic approximation they determined that the quantity $\frac{\partial}{\partial y^*} \left[\rho^* \frac{\partial u^*}{\partial y^*} \right]$ (where u^* denotes velocity tangential to the surface, y^* the normal to the surface, and ρ^* the fluid density) plays a key role, similar to that the quantity $\partial^2 u^* / \partial y^{*2}$ has in incompressible theory. In particular at the point where the above expression is zero ($y^* = y_i^*$), termed the generalised inflexion point, then there may exist a neutral mode with wavespeed $u^*(y_i^*)$; neutral modes are classed as being 'subsonic', 'sonic' or 'supersonic' depending on how the freestream Mach number is related to the wavespeed (Mack (2)). If the neutral disturbance is subsonic then the mode decays in the far-field; supersonic, neutral disturbance modes exhibit an oscillatory behaviour in the far-field;

a sonic mode occurs at the crossover point between subsonic and supersonic cases. Mathematically, these classifications are directly related to the non-dimensional wavespeed c (defined in (2.10) below), and the free-stream Mach number M_∞ . For subsonic disturbances we have

$$1 - \frac{1}{M_\infty} < c < 1 + \frac{1}{M_\infty} ,$$

for sonic disturbances we have

$$c = 1 - \frac{1}{M_\infty} \text{ or } c = 1 + \frac{1}{M_\infty} ,$$

and for supersonic disturbances we have

$$c < 1 - \frac{1}{M_\infty} \text{ or } c > 1 + \frac{1}{M_\infty} .$$

Arguments relating to generalised inflexion points have no implications for supersonic neutral modes.

Lees (3) considered the effect that wall cooling has on the stability of compressible boundary layers on the basis of asymptotic theory. He predicated that with sufficient wall cooling the boundary layer could be completely stabilized and presented a criterion whereby the ratio of wall temperature to the recovery temperature at which the critical Reynolds number becomes infinite, can be computed. Even though Lee's original work contained numerical errors, subsequent authors including Van Driest (4) and Dunn and Lin (5) showed that Lee's predictions appeared to be correct.

Van Driest (4) calculated the cooling required to completely stabilize the boundary layer on a flat plate at supersonic speeds with zero pressure gradient. Whereas Lee's investigations were limited to low supersonic flows, Van Driest predicated that complete stabilization was achievable by wall cooling over a wide range of Mach numbers up to hypersonic flow. He found, however, that for Mach numbers greater than 9,

it is impossible to stabilize the boundary layer with any amount of cooling when a Prandtl number of 0.75 and the Sutherland viscosity-temperature law are assumed.

The above predictions of Lees (3) and Van Driest (4) were based on the asymptotic theory of two-dimensional disturbances. Dunn and Lin (5) extended this work to include three-dimensional disturbances and they indicated that cooling was indeed an effective method by which the boundary layer could be stabilized for moderate supersonic Mach numbers. Based on their asymptotic analysis, Dunn and Lin, however (wrongly) concluded that at supersonic free-stream Mach numbers the boundary layer can never be completely stabilized by cooling with respect to all three-dimensional disturbances.

However the above asymptotic work is found to have its limitations. The theory above indicates the possible existence of only subsonic generalised modes for cooled wall conditions. In a series of papers Mack (2, 6, 7, 8, 9, 10, 11), using numerical techniques, demonstrated that for compressible boundary layers there in actual fact exist a large (probably infinite) number of unstable modes, including many with supersonic neutral points, which may not be predicated by the above asymptotic work. For the case of three-dimensional disturbances in Blasius-type boundary layers, Mack showed that the so-called ''first mode'' of instability undergoes stabilization with sufficient wall cooling, thus verifying the above mentioned asymptotic analysis. However, Mack found in the case of the ''second mode'' of instability (which turns out to be more important because of the larger growth rates involved) cooling the wall actually destabilizes this mode. According to recently presented numerical observations by Mack (2, 10) oblique disturbances can be completely stabilized by wall cooling for Mach numbers up to 5.8, although they do require a larger amount of cooling than the corresponding two-dimensional disturbance terms.

Recently, Duck (12), considering the effect of curvature on the inviscid axisymmetric stability of a compressible boundary layer, determined that it has a profoundly stabilizing effect. Considering axisymmetric, inviscid disturbances in the supersonic boundary layer formed on a thin straight circular cylinder with adiabatic wall conditions, he determined that the effect of curvature is to completely stabilize the ''first mode'' of inviscid instability at a comparatively short distance down the axis of the cylinder and causes the ''second mode'' of instability to undergo substantial maximum growth rate reductions at increasingly further downstream locations along the cylinder axis. All the numerical evidence though, is that for large distances downstream the ''second mode'' is still present, having a very small, but measurable growth rate. Duck also observed that the inclusion of curvature terms causes the generalised inflexion condition described above to be altered and he derived a modified (or ''doubly generalised'') inflexion condition, involving the radius of curvature.

The work of Duck (12) was extended to include non-axisymmetric disturbance terms by Duck and Shaw (13) (here-after referred to as DS) and they applied their techniques to a different axisymmetric configuration, namely that of a sharp cone. DS generalised the doubly generalised inflexion condition further, to give a condition for the existence of so called inviscid, neutral non-axisymmetric modes and termed it the ''triply generalised inflexion condition''.

In this paper we consider the combined effects that curvature and wall cooling (or heating) have on the stability of the compressible boundary layer associated with an axisymmetric body (principally a thin, straight circular cylinder). We are interested in both axisymmetric and non-axisymmetric, inviscid disturbances. The theory for the form of the

boundary layer and the resultant disturbance equations has already been presented by Duck (12) and in DS, to which we refer the reader to for details, but we shall begin this paper with a brief account of the relevant equations to the present problem. It should be noted that although the work in DS was for a sharp cone, the necessary equations for a circular cylinder for this problem are easily obtained by setting the slope parameter, λ in DS to zero.

§2 Formulation of Problem

The general layout of the problem is shown in Figure 1. The z^* axis lies along the cylinder axis, r^* denotes the radial coordinate, and θ the azimuthal coordinate. We have a supersonic flow incident normal on the end-face of the cylinder (which has radius a^*), where M_∞ represents the free-stream Mach number, U_∞^* the free-stream velocity (in the axial direction) and ρ_∞^* , μ_∞^* and T_∞^* represents the free-stream density, first coefficient of viscosity and temperature respectively. We define the Reynolds number to be

$$Re = \frac{U_\infty^* a^* \rho_\infty^*}{\mu_\infty^*}, \quad (2.1)$$

and this will be assumed to be large throughout. Subscript ∞ denotes free-stream conditions.

For the resultant boundary layer formed on the cylinder we make the following assumptions:-

Firstly following previous authors we shall assume an absence of any shock wave in the basic flow. We feel justified in making this assumption, as the chosen 'thinness' of the boundary layer is such that the shock wave will be sufficiently far away from the boundary layer to have negligible effect. Secondly we shall assume the linear Chapman viscosity law, where

$$\mu^* = C T^*, \quad (2.2)$$

and C is assumed to be constant. Since the flow is one of high

Reynolds number, we make the steady boundary-layer approximation. A fundamental component of this work is the inclusion of curvature terms into the governing equations. To achieve this we assume that the body radius is generally of the same order as the boundary-layer thickness (a similar approach was adopted by Seban and Bond (14), Duck and Bodonyi (15), Duck (12) and in DS), except at the tip of the cylinder where we shall assume the boundary layer has zero thickness (as assumed by Seban and Bond (14)). The final assumption we shall make is that of a perfect gas.

Making use of the above mentioned assumptions, in DS, we obtained the following system of non-dimensional, leading order equations for the basic flow

$$\frac{\partial}{\partial r} \left[\frac{v_1}{T} \right] + \frac{v_1}{rT} + \frac{\partial}{\partial z} \left[\frac{v_3}{T} \right] = 0, \quad (2.3)$$

$$\frac{\partial P}{\partial r} = 0, \quad (2.4)$$

$$v_1 \frac{\partial v_3}{\partial r} + v_3 \frac{\partial v_3}{\partial z} = \frac{T}{r} \frac{\partial}{\partial r} \left[r T \frac{\partial v_3}{\partial r} \right], \quad (2.5)$$

$$v_1 \frac{\partial T}{\partial r} + v_3 \frac{\partial T}{\partial z} = T^2 (\gamma - 1) M_\infty^2 \left(\frac{\partial v_3}{\partial r} \right)^2 + \frac{T}{r} \frac{\partial}{\partial r} \left[\frac{r}{\sigma} T \frac{\partial T}{\partial r} \right], \quad (2.6)$$

where $U_\infty^* (Re^{-1} C v_1, v_2, v_3)$ represent the velocity components in the $(r^* = a^* r, \theta, z^* = Re a^* C^{-1} z)$ directions respectively, $p^* R^* T^* P$ (where R^* is the gas constant) and $T_\infty^* T$ represent the pressure and temperature terms respectively, γ denotes the ratio of specific heats and $\sigma = \frac{\mu}{K^*} C_p$ is the Prandtl number, with K^* being the coefficient of heat conductivity; in (2.3)-(2.6) the basic flow is assumed independent of θ , and has no azimuthal velocity component (i.e. $v_2 = 0$).

The boundary conditions for the problem are

$$\begin{aligned} v_1 = v_3 = 0 \quad \text{on } r=1, \\ v_3 \rightarrow 1, T \rightarrow 1 \quad \text{as } r \rightarrow \infty, \end{aligned} \quad (2.7)$$

together with a wall temperature condition which for heated or cooled walls

has the form

$$T = T_w \text{ on } r=1. \quad (2.8)$$

The system of equations (2.3)-(2.6) was solved using a straight-forward Crank-Nicolson scheme, as described in DS, subject to the boundary conditions (2.7) and (2.8).

To study the stability of this basic flow, we now investigate the effect of small amplitude disturbances. We shall assume that the disturbance wavelength is generally comparable to the boundary-layer thickness and therefore also of the body radius ($O(a^*)$), in which case the parallel flow approximation is completely vindicated.

At a fixed z -station we express the flow parameters of velocity, pressure, temperature and density as the sum of a mean flow term plus a small, first order disturbance term, for example,

$$\begin{aligned} v_1^* &= \delta \alpha U_\infty^* \varphi(r) E + O(\delta^2), \\ v_3^* &= U_\infty^* [w_0(r) + \delta \tilde{v}_3(r)E] + O(\delta^2), \\ T^* &= T_\infty^* [T_0(r) + \delta \tilde{T}(r)E] + O(\delta^2), \\ P^* &= \rho_\infty^* R^* T_\infty^* [1 + \delta \tilde{p}(r)E] + O(\delta^2), \end{aligned} \quad (2.9)$$

where

$$E = \exp\left[\frac{i\alpha}{\zeta} (\hat{z} - ct) + i n \theta\right], \quad (2.10)$$

$$\begin{aligned} T_0(r) &= T(r, z) \\ w_0(r) &= v_3(r, z) \end{aligned} \quad (2.11)$$

and

$$\zeta = z\frac{1}{a^*}, \quad \eta = (r-1)/\zeta, \quad \hat{z} = z^*/a^*, \quad (2.12)$$

and δ is the perturbation parameter and as such is assumed to be diminishingly small.

In this paper we focus our attention on temporal stability for which the growth rate is αc_i , where α represents the spatial wavenumber and c_i is the imaginary part of the wavespeed. If $c_i > 0$ we then have growing disturbances, if $c_i = 0$ the disturbance is neutral and if

$c_i < 0$ the disturbance decays.

Substitution of the flow parameters into the full system of equations of continuity, momenta, energy and state, discarding $O(\delta^2)$ terms and all but the largest terms in Re , we obtain a sixth order system, which after some algebra (as described in DS) can be reduced to the following system

$$\frac{i\alpha^2(w_0-c)}{T_0} \varphi = - \frac{\tilde{p}_\eta}{\gamma M_\infty^2}, \quad (2.13)$$

$$\frac{i\tilde{p}}{\gamma M_\infty^2} \varphi = (w_0-c)\varphi_\eta - [w_0\eta - \frac{(w_0-c)\zeta}{1+\eta\zeta}]\varphi, \quad (2.14)$$

where

$$\Phi = T_0 \left[1 + \frac{n^2\zeta^2}{\alpha^2(1+\eta\zeta)^2} \right] - M_\infty^2(w_0-c)^2. \quad (2.15)$$

The boundary conditions are

$$\varphi = \tilde{p}_\eta = 0 \quad \text{on} \quad \eta = 0, \quad (2.16)$$

and

$$\left. \begin{aligned} \varphi &\sim \varphi_\infty K_n(\hat{\eta}) \\ \tilde{p} &\sim \tilde{p}_\infty K_n(\hat{\eta}) \end{aligned} \right\} \quad \text{as } \eta \rightarrow \infty, \quad (2.17)$$

where

$$\hat{\eta} = \pm \alpha[1-M_\infty^2(1-c)^2]^{\frac{1}{2}} \left(\frac{1}{\zeta} + \eta \right). \quad (2.18)$$

It should be noted that the argument of the modified Bessel function (i.e. appropriate sign in (2.18)) $K_n(\hat{\eta})$ is chosen to ensure boundedness in the farfield.

The system of equations (2.13), (2.14) was solved using a Runge-Kutta scheme for the eigenvalue c , as described in DS, subject to the boundary conditions (2.16), (2.17).

§3 Numerical Results

Most of this section will be devoted to the effect of wall-cooling on the stability of compressible boundary layers and its interaction with curvature, as these conditions are likely to be of interest in important applications. However, at the end of the section we shall give some heated wall results which exhibit some additional interesting physical features.

As in DS we shall make one choice of Prandtl number ($\sigma=0.72$), Mach number ($M_\infty=3.8$) and ratio of specific heats ($\gamma=1.4$).

3.1. Cooled Wall Results

We begin by considering the effect that wall cooling has on the inflexion points. In DS a condition was derived for the existence of inviscid, neutral, non-axisymmetric modes in the boundary layer on an axisymmetric body, which was termed the 'triply generalised inflexion condition'. However this condition does involve the azimuthal and streamwise wavenumbers α and n , and so it is difficult to forecast, prior to any numerical investigation, the existence of neutral stability points of this kind. However in the case of axisymmetric disturbances, this is no longer the case, since the condition reduces to

$$\frac{d}{dr} \left[\frac{w_{0r}(r)}{rT_0(r)} \right] = 0, \quad (3.1)$$

as determined by Duck (12).

Figure 2a shows the axial variation of radial position of the generalised inflexion points for the temperatures shown. As in the insulated cylinder case (12), the graphs display two prominent features: (i) the inflexion points occur in pairs and (ii) there exists a critical value of ζ , downstream of which no such points exist. The point $\zeta = 0$ corresponds to the tip of the cylinder and as such corresponds to the planar case as studied by Mack (2). We find that as the surface of the cylinder is cooled, the lower inflexion point lifts up off the

cylinder surface. For sufficient cooling the lower point coalesces with the upper inflexion point and further cooling results in the complete disappearance of the inflexion points. Therefore for a given ζ -station there exists a critical wall temperature below which no inflexion points exist. In light of our earlier comments, we do have an additional condition for the existence of neutral subsonic disturbances, namely that

$$1 - \frac{1}{M_\infty} < c < 1 + \frac{1}{M_\infty}. \quad (3.2)$$

This has direct implications on the first mode of instability as this generally requires the presence of an inflexion point in the profile satisfying (3.2).

Figure 2b shows the axial variation of $w_0(\eta_i)$ for the displayed wall temperatures. From stability theory, unstable subsonic modes only exist if a generalised inflexion point satisfying (3.2) occurs somewhere in the boundary layer. Examination of the curve for $T_w = 3.0$ reveals that subsonic generalised inflexion points only occur for $0 \leq \zeta \leq 0.0795$; consequently the mode has completely disappeared before the generalised inflexion points have merged. For a wall temperature of $T_w = 2.0$ the generalised inflexion points are all now supersonic in nature ($c < 1 - \frac{1}{M_\infty}$), implying for this and all cooler wall temperatures the eradication of Mode I instabilities.

We now turn our attention to the eigenvalue problem for both axisymmetric and non-axisymmetric disturbances. We shall present only results for unstable modes and all plots are for c_i (where $c = c_r + ic_i$). The first set of results we present corresponds to the tip of the cylinder and as such are comparable to the planar results as obtained by Mack (2, 10, 11). Figure 2c displays distributions for the first mode of instability. We observe that all the modes originate as sonic (i.e. with $c = 1 - \frac{1}{M_\infty}$) neutral modes and terminate as subsonic, generalised inflexional modes. We note that as we cool the surface of the cylinder

this mode undergoes stabilization, until, with sufficient cooling it becomes completely stable, thus verifying Mack's observations (and those of Lees (3), Van Driest (4) and Dunn and Lin (5)). From our inflexion point results, this is to be expected, as we observed that for cool enough wall conditions, $w_0(\eta_i)$ drops below $1 - \frac{1}{M_\infty}$ and we no longer have the necessary conditions for a subsonic generalised inflexional mode.

Figure 2d shows the second mode of instability at the tip of the cylinder. All the modes originate as subsonic generalised inflexional modes with the special case $c(=c_r = w_0(\eta_i)) = 1$, which therefore corresponds to a generalised inflexion point in the freestream, and terminate as neutral modes. Depending on whether or not a subsonic generalised inflexional mode for the given wall conditions exists, this neutral mode is either subsonic inflexional or supersonic, in nature, and the mode may continue as a decaying mode ($c_i < 0$). Examination of our results reveals that as we cool the cylinder surface, the maximum value of c_i increases slightly and then decreases but the important product αc_i , actually increases with wall cooling. Thus we deduce that wall cooling destabilises the second mode of instability, in line with Mack's (2, 10, 11) observations.

The next set of results we present corresponds to a relatively small distance from the tip along the cylinder in the axial direction, at the location $\zeta = 0.05$, and for an axisymmetric mode (ie, $n=0$). Figure 2e displays the Mode I distributions and we note that with sufficient cooling, it is again possible to completely stabilize this mode. We observe that the neutral mode at which this instability originates now occurs for α slightly greater than zero and it is very slightly supersonic in nature. When compared with the corresponding planar results we note that curvature (as noted by Duck (12) and DS) has a profoundly stabilizing effect. Even though this station is only a relatively short distance along the cylinder

from the tip, curvature has reduced the value of maximum c_i for the $T_w = 3.0$ curve by a factor of 4, while for the $T_w = 2.8$ curve this factor is almost 5. Curvature results in the mode requiring less cooling to completely stabilize it. Figure 2f displays the axisymmetric mode II instability at this axial location. Again we note that curvature has had a stabilizing effect on the instability, but cooling causes the mode to become more unstable, in line with the planar results described previously.

The next set of results we present corresponds to the $\zeta=0.05$ location, for azimuthal wavenumber $n=1$. Figures 2g, 2h display the mode I and II instabilities, respectively. We observe that in this case the mode I instability is substantially more unstable than the axisymmetric case. We find again, however, with sufficient cooling we can completely stabilize this mode, although the mode does persist for cooler wall conditions. The mode II instability has the same qualitative features as the axisymmetric case, although it is slightly more stable than the axisymmetric case.

In DS it was noted that near the cone tip, for non-axisymmetric disturbance terms, a third mode of instability is seen to develop. This new mode originates as a neutral mode at $\alpha=0$, with $c_i \neq 0$, terminates as a supersonic neutral mode and was termed in DS, mode IA. As has already been noted, the work of DS was for a cone with adiabatic wall conditions and it was found that this new mode had already amalgamated with mode I instability at the $\zeta=0.05$ location for $n=1$. We find however that for a cooled cylinder at this axial location and $n=1$, the mode IA instability is still distinct (Figure 2i) over the range of T_w shown; a possible partial explanation is provided in Section 6. We observe that wall cooling causes mode IA instability to become less unstable and with sufficient wall cooling we can completely stabilize it. Comparing with the mode I instability we note that the maximum value of c_i for the mode IA instability is an order of magnitude larger, but due to the smallness of α ,

the mode I growth rates are generally larger. One further observation, though, is that mode IA instability persists for cooler wall temperatures than does the mode I instability.

We now consider the situation for an azimuthal wavenumber of $n=3$, at this axial location. We observe that for this case the mode I and IA instabilities have now amalgamated. The new combined mode originates as a neutral mode (but with $c_i \neq 0$ for $\alpha=0$) and terminates as a subsonic generalised inflexional mode (Figure 2j). Again we note that sufficient wall cooling can completely stabilize this mode, although it is found that this mode persists for cooler wall temperatures as n increases. Comparing with the $n=1$ results we find that the increase in n has also caused the mode to become slightly less unstable. The mode II instability (Figure 2k), again, has the same qualitative features, but has also undergone stabilization with the increase in n . However, it is found that cooling has the more dominant destabilizing effect here.

The next set of results we present correspond to an azimuthal wavenumber of $n=5$, at this axial location. We observe the same qualitative features as the $n=3$ results for both modes (Figures 2l, 2m), although we note that we have had a more significant stabilizing effect due to the increase in n . The mode I instability is now completely stabilized for higher wall temperatures, while again, it is observed that cooling causes an even more marked destabilizing effect for the mode II instability.

We find that as the azimuthal wavenumber n is further increased, both the mode I and II instabilities undergo additional stabilization, although cooling maintains a destabilizing effect on Mode II. For large n it is found that Mode I instability is completely stabilized while the mode II instability persists, but with much diminished growth rates. In the next section we shall consider the asymptotic structure of the disturbance equations in this limit.

The final set of results we shall present in this sub-section corresponds to the axial location $\zeta=0.5$ and for an azimuthal wavenumber of $n=1$. We find that at this distance along the cylinder the mode I and IA instabilities have now combined (Figure 2n). Comparison with the $n=1$ results at the $\zeta=0.05$ location, we note that growth rates have been reduced due to the stabilizing effect of curvature. It is found, however, that the combined mode prevails for cooler wall conditions, but again is completely stabilized with sufficient wall cooling. Figure 2o displays the mode II instability. Curvature has resulted in the growth rates being reduced, but we observe that cooling has a more profound destabilizing effect here.

As we move further along the cylinder in the axial direction, the mode I and II instabilities undergo further growth-rate reductions. For a given wall temperature, T_w , azimuthal wavenumber n , axial wavenumber α , there exists a critical value of ζ , beyond which no triply generalised inflexion points (see DS for details) occur. Consequently, we expect the mode I instability to have disappeared for axial distances larger than this critical ζ , which is borne out by our numerical results. It is found however that due to the special nature of the inflexional point within the freestream, the mode II instability still originates with $c=1$, even for axial distances greater than this critical ζ , although the mode has much reduced growth rates. In the light of this, in Section 5 we shall consider the form of the disturbance equations in the limit of large ζ .

3.2 Heated Wall Results

We begin by considering the effect that wall heating has on the inflexion points. We restrict our study to the case of axisymmetric disturbances, and consider the effect wall heating has on condition (3.1).

Figure 3a shows the axial variation of (radial) position of the generalised inflexion points for the temperatures shown. We observe again the features seen in Figure 2a. Close to the cylinder tip, however, we find that for a small axial distance measured from the tip, we no longer have any lower inflexional points. As we heat the surface of the cylinder further, this axial distance is found to increase. It is also observed that wall heating causes the critical value of ζ , beyond which no inflexional points exist, to increase. For $T_w=4.5$, the critical value of ζ is about 0.216, while for $T_w=6.0$, we have had a substantial increase to a value of $\zeta \approx 0.423$. This will have direct implications on the first mode of instability which we expect to persist for larger axial distances as the wall is heated. These effects are in many ways to be expected, being the converse of the cooling observations described earlier.

Figure 3b shows the axial variation of $w_0(\eta_i)$ for the displayed wall temperatures. The most marked feature of these curves is that as we heat the cylinder surface, the lower inflexional point becomes subsonic past a critical value of ζ , which is temperature dependent, i.e. for axial distances greater than this critical value of ζ but upstream of the station beyond which no inflexional points occur, both generalised inflexional points are now subsonic in nature. The first wall temperature for which we observe a lower, subsonic inflexional point is for a wall temperature of about $T_w=4.5$. It is found, however, that the critical value of ζ here, is very close to the stations where the generalised inflexional points coalesce. For $T_w=5.0$ we observe that for the range $0.2635 \leq \zeta \leq 0.2720$ we have two subsonic inflexional modes, while for the hotter wall temperature of $T_w=6.0$ we have the larger range $0.363 \leq \zeta \leq 0.423$ for which both generalised

inflexional points are subsonic. In these ζ -ranges we expect the appearance of two subsonic generalised inflexional modes to have a significant effect on the physics of the problem.

We now present eigenvalue results for axisymmetric disturbances only. As in the case of cooled wall conditions we focus attention on unstable modes. We begin by considering the effect wall heating has on the mode I and II instabilities for a ζ -station close to the cylinder tip ($\zeta=0.05$) and consequently the lower inflexional point is still supersonic in nature. Figure 3c shows the mode I instability for the temperatures shown. We observe that all the modes originate as neutral modes at a value of α slightly greater than zero, and are very slightly supersonic in nature. We find as we heat the wall this neutral mode tends towards the sonic value. All the modes terminate as subsonic generalised inflexional modes, continuing on as stable modes ($c_i < 0$) for larger values of α . These observations are similar to the results obtained for the axisymmetric cooled wall case for this ζ -station. We find, as we would expect, heating the surface of the cylinder causes the mode I instability to become more unstable - converse to the effect of cooling on this mode.

Figure 3d displays the mode II instabilities for the $\zeta=0.05$ station, at the temperatures shown. We find all the modes originate as subsonic generalised inflexional modes, rise to a maximum and terminate as subsonic generalised inflexional modes (which then continue in all the cases presented as stable modes). Heating the cylinder wall causes the mode II instability to become less unstable and the numerical evidence suggests that with sufficient heating we can completely stabilize this mode.

We now consider the effect that the lower inflexional point becoming subsonic has on the mode I and II instabilities. Figure 3e displays the mode I instability for a wall temperature of $T_w=5.0$ and for the

ζ -stations as marked. For the $\zeta=0.26$ station (where the lower inflexional point is still supersonic) the mode originates as a very slightly supersonic mode and terminates as a subsonic generalised inflexional mode. For the $\zeta=0.264$ station the lower inflexional point has now become subsonic in nature, and we find the mode I instability now originates as this lower subsonic generalised inflexional mode. Consequently the value of α for the neutral mode has increased correspondingly. As before, the mode I instability terminates as the upper generalised inflexional mode which is of course subsonic, as well. From the inflexional point curves we know that as we move upstream the inflexional points move closer together, eventually coalescing and this is reflected in the new form of the mode I instabilities. For the $\zeta=0.27$ station the mode I instability occurs over a much smaller α -range and the growth rates are greatly reduced.

Figure 3f displays the mode I instability for a wall temperature of $T_w=6.0$ and the displayed ζ -stations. Again we note that as the lower inflexional point becomes subsonic the neutral point at which the instability originates transforms from being very slightly supersonic in nature, to this inflexional mode. Movement upstream causes the α -ranges and growth rates to be diminished, but the reduction is less marked (in comparison with the $T_w=5.0$ results) due to the destabilizing effect brought on by wall heating.

The appearance of a second subsonic generalised inflexional mode is found to have no effect on the mode II instability as it always terminates as the upper generalised inflexional mode. It is found, however, that a third mode of instability exists, originating as the lower generalised inflexional mode and terminating as a slightly supersonic neutral mode. This new mode, which we shall term Mode IIA, occurs for values of α greater than the value of α for which the mode II instability terminates. It appears that the mode II instability continues as a stable mode and

then becomes unstable again at the lower generalised inflexional point. The growth rates of the mode IIA are found to be very small. For a wall temperature of $T_w=5.0$ and the station $\zeta=0.27$ the growth rates are in the order 10^{-11} , while for $T_w=6.0$ and $\zeta=0.364$ the growth rates are of the order of $10^{-13} - 10^{-14}$.

We now move on to consider the form of the disturbance equations in the limit of large azimuthal wavenumbers.

§4. Disturbance Equations for Large n

In this section we consider the form of the disturbance equations in the asymptotic limit of large n , guided by our numerical results.

4.1 Formulation of the Problem

Consider the pressure disturbance equation as derived in DS

$$\frac{w_0-c}{\alpha^2} \frac{d}{d\eta} \left[\frac{T_0 P_n}{w_0-c} \right] + \left[\frac{(w_0-c)\zeta}{1+\eta\zeta} - w_0\eta \right] \frac{T_0 P_n}{\alpha^2(w_0-c)} = \Phi P, \quad (4.1)$$

where

$$\Phi = T_0 \left[1 + \frac{n^2 \zeta^2}{\alpha^2(1+\eta\zeta)^2} \right] - M_\infty^2 (w_0-c)^2. \quad (4.2)$$

In the limit of large n our numerics suggest that the corresponding streamwise wavenumbers for the instability also increase, and that $\Phi(\eta=0) \rightarrow 0$. Equation (4.2) suggests we must have

$$\alpha = \bar{\alpha}n, \quad \bar{\alpha} = O(1). \quad (4.3)$$

A (sensible) balancing of terms in equation (4.1) suggests asymptotic expansions of the form

$$\begin{aligned} c &= c_0 + n^{-2/3} c_1 + O(n^{-4/3}) + \dots, \\ \Phi &= \Phi_0 + n^{-2/3} \Phi_1 + O(n^{-4/3}) + \dots. \end{aligned} \quad (4.4)$$

The leading order pressure equation has the form

$$P_{\eta\eta} - \frac{\alpha^2}{T_0} \Phi_0 P = 0, \quad (4.5)$$

where

$$\Phi_0 = T_0 \left[1 + \frac{\zeta^2}{\alpha^2 [1 + \eta \zeta]^2} \right] - M_\infty^2 (w_0 - c_0)^2. \quad (4.6)$$

This has a solution of the (bounded) WKB type (assuming $\text{Im}\{(-\Phi_0)^{1/2}\} > 0$)

$$P = \frac{P_0}{\Phi_0^{1/2}} \left\{ i \frac{\alpha}{T_0^{1/2}} \int^\eta [-\Phi_0]^{1/2} d\eta \right\}. \quad (4.7)$$

We can re-write the expansion for Φ in the neighbourhood of $\eta = 0$ as

$$\Phi = \Phi_0(0) + n^{-2/3} [\Phi_0'(0) \bar{\eta} + \Phi_1(0)] + O(n^{-4/3}), \quad (4.8)$$

where

$$\Phi_0(0) = T_w \left[1 + \frac{\zeta^2}{\alpha^2} \right] - M_\infty^2 c_0^2, \quad (4.9)$$

$$\Phi_1(0) = -2 c_0 c_1 M_\infty^2, \quad (4.10)$$

and for insulated wall conditions

$$\Phi_0'(0) = -\frac{2 \zeta^3 T_w}{\alpha^2} + 2 M_\infty^2 w_0'(0) c_0, \quad (4.11)$$

while for heated or cooled wall conditions we have

$$\Phi_0'(0) = T_{0\eta}(0) \left[1 + \frac{\zeta^2}{\alpha^2} \right] - \frac{2 \zeta^3 T_w}{\alpha^2} + 2 M_\infty^2 w_0'(0) c_0, \quad (4.12)$$

where T_w represents the wall temperature.

If $\Phi_0(0) = 0$, then we must have

$$c_0 = \frac{T_w^{1/2} \left[1 + \frac{\zeta^2}{\alpha^2} \right]^{1/2}}{M_\infty} \quad (4.13)$$

(which is clearly real). We now seek to determine the first order

correction term to c , namely c_1 . For this we must study the wall layer, which by a balancing of terms of (4.2) suggests is given by

$$\eta = \bar{\eta} n^{-2/3}, \quad \bar{\eta} = O(1). \quad (4.14)$$

The (bounded) solution for P in the wall layer is given by

$$P = \hat{P}_0 \text{Ai}(\tilde{\eta}), \quad (4.15)$$

where \hat{P}_0 is a constant and $\tilde{\eta}$ is given by

$$\tilde{\eta} = \left\{ \frac{\bar{\alpha}^2}{T_w[\phi_0'(0)]^2} \right\}^{1/3} [\phi_0'(0)\bar{\eta} + \phi_1(0)]. \quad (4.16)$$

The boundary condition at the wall is

$$P_\eta \big|_{\eta=0} = 0. \quad (4.17)$$

which we transform to $\tilde{\eta}$ -space, giving the equation

$$P_{\tilde{\eta}} [\tilde{\lambda}^{-1/3} \tilde{\eta} = B] = 0, \quad (4.18)$$

where

$$\tilde{\lambda} = \frac{\bar{\alpha}^2}{T_w[\phi_0'(0)]^2}, \quad B = \phi_1(0). \quad (4.19)$$

Now since the solution in this region to the pressure is given by Airy's function (4.15) we have that

$$\text{Ai} \tilde{\eta} [\tilde{\eta} = B \tilde{\lambda}^{1/3}] = 0. \quad (4.20)$$

Transforming back to η -space we have the result

$$\gamma_n = \left\{ \frac{\bar{\alpha}^2}{T_w[\phi_0'(0)]^2} \right\}^{1/3} [-\phi_1(0)], \quad (4.21)$$

where γ_n (where $n = 1, 2, \dots$) represent the solutions of the equation

$$\text{Ai}'(-\gamma_n) = 0. \quad (4.22)$$

Substituting either (4.11) or (4.12) and equation (4.10) into equation (4.21) yields the first order correction term for c_1 namely

$$c_1 = \frac{T_w^{1/3} \left\{ 2 [M_\infty^2 w_0'(0) c_0 - \frac{T_w \zeta^3}{\bar{\alpha}^2}] \right\}^{2/3}}{2 \bar{\alpha}^{2/3} M_\infty^2 c_0} \gamma_n, \quad (4.23)$$

for insulated walls, whilst for heated/cooled wall conditions we have

$$c_1 = \frac{T_w^{1/3} \left\{ 2 [M_\infty^2 w_0'(0) c_0 - \frac{T_w \zeta^3}{\bar{\alpha}^2}] + T_0'(0) \left[1 + \frac{\zeta^2}{\bar{\alpha}^2} \right] \right\}^{2/3}}{2 \bar{\alpha}^{2/3} M_\infty^2 c_0} \gamma_n, \quad (4.24)$$

where c_1 is real for both cases.

Since γ_n is a solution of equation (4.22), where $\gamma_n > 0$, then we have an infinite number of discrete, real possible values for γ_n as the derivative of the Airy function has an infinite number of discrete roots, confined to the negative real axis. This suggests that there are an infinite number of modes.

We shall now compare these results with numerically determined results for large values of n .

4.2 Numerical Results

All the results presented in this section are for a freestream Mach number of 3.8 and at the point $\zeta = 0.2$ along the cylinder. We only present results for adiabatic wall conditions.

Firstly let us consider the asymptotic expansion for c in the limit of large n . The leading order term in the c expansion c_0 , is given by equation (4.13) and using the numerically determined values

$$T_w = 3.379, \quad (4.25)$$

$$\bar{\alpha} \approx 0.1525,$$

we have

$$c_0 \approx 0.7978. \quad (4.26)$$

The first order correction term, which for adiabatic wall conditions is given by equation (4.23), is computed to have the value

$$c_1 \approx 0.3698 \gamma_n, \quad (4.27)$$

where we have used $w_{0\eta}(0) \approx 0.1904$ and γ_n are the zeros of the derivative of the Airy function. The first six possible values of γ_n are determined from tables (Abramowitz & Stegun (16)) and the corresponding values of c_1 are shown in table I

c_1	
0.3698	(I)
1.2092	(II)
1.7750	(III)
2.5146	(IV)
2.9214	(V)
3.3282	(VI)

TABLE I: VALUES OF c_1

Figure 4a shows a plot of $c(=c_0 + n^{-2/3} c_1)$, as determined asymptotically, against n for the different values of the first order correction term c_1 , where the numbering refers to the numbering of the correction terms in Table I. (It should be noted that only n integer has physical significance, although Figs. 4a and 4b show c as a continuous function of n .) From hereon we shall refer to the different values of c as order I to VI inclusively corresponding to the numbering convention of the correction terms in Table I.

Now as observed above, our asymptotic analysis suggests the existence of an infinite, discrete number of possible values for c . When we searched for the eigenvalues numerically, for large n , we determined that there were indeed many modes. Figure 4b displays two plots of c_r against n for order I and order V correction terms. Graph (1) in each case represents

the asymptotic curve and graph (2) is the numerically determined curve. It should be noted that in this range of n and α , $|c_i| \ll 1$ ($c_i \sim 10^{-10} - 10^{-12}$), comparable to the machine accuracy of our computations. From our two sets of plots we note that we have good agreement between the numerical solutions and asymptotic theory for large n .

Turning our attention now to the form of the pressure disturbance terms, as obtained numerically, we find that they do indeed follow the pattern predicated by our asymptotic theory, being initially oscillatory in the Airy solution region and then decaying to zero in the far field. It is also observed that increasing the order of the correction term has the effect of increasing the number of zeros of the eigensolution. Figure 4c displays the distributions of Real (P) for $n = 40$ corresponding to the orders as shown.

Examining the c expansion again, we have determined that both c_0 and c_1 are real and therefore the leading order imaginary term, c_i , is at most $O(n^{-4/3})$. This means that the leading order term in the growth rate ($\propto c_i$) is $O(n^{-1/3})$ at most. Therefore actual growth rates will decrease as $n \rightarrow \infty$ which is confirmed to be true by our numerical observations.

We now turn our attention to the form of the disturbance equations in the limit $\zeta \rightarrow \infty$.

§5 Disturbance Equations for Large ζ

In this section we consider the form of the disturbance equations in the far downstream region, guided by our numerical observations.

5.1 Formulation of the Problem

Consider the pressure disturbance equation, as presented in the previous section, but written in terms of ' r ' rather than ' η ',

$$\frac{w_0 - c}{\alpha^2} \frac{d}{dr} \left[\frac{T_0 P_r}{w_0 - c} \right] \zeta^2 + \left[\frac{w_0 - c}{r} - w_{0r} \right] \frac{T_0 P_r \zeta^2}{\alpha^2 (w_0 - c)} = \Phi P, \quad (5.1)$$

where

$$\Phi = T_0 \left[1 + \frac{n^2 \zeta^2}{\alpha^2 r^2} \right] - M_\infty^2 (w_0 - c)^2, \quad (5.2)$$

and

$$r = 1 + \eta \zeta. \quad (5.3)$$

In the limit $\zeta \rightarrow \infty$, we assume a scale of α of the form

$$\alpha = \bar{\alpha}^+ \zeta, \quad (5.4)$$

where $\bar{\alpha}^+$ is to be determined.

Guided by Duck's (12) work for the form of the basic flow in the farfield we define the (small) parameter

$$\epsilon = (\frac{1}{2} \log Z)^{-1} = (\log \zeta)^{-1}. \quad (5.5)$$

In the slow moving viscous region close to the wall (namely the $r=O(1)$ lengthscale) we expect asymptotic expansions of the form

$$\begin{aligned} c &= \hat{c}_0 + \epsilon \hat{c}_1 + O(\epsilon^2), \\ \Phi &= \hat{\Phi}_0 + \epsilon \hat{\Phi}_1 + O(\epsilon^2), \\ T_0 &= T_w + \epsilon T_1 + O(\epsilon^2), \\ w_0 &= \epsilon \bar{w}_0 + O(\epsilon^2). \end{aligned} \quad (5.6)$$

Now, our numerical observations strongly suggest that $\hat{\Phi}_0 \rightarrow 0$ as ζ becomes large in the $r = O(1)$ region (which may be confirmed a posteriori) which means that $\Phi = O(\epsilon)$. Examination of the Φ expression reveals that this is only possible in general if

$$\bar{\alpha}^+ = O(\epsilon^{-\frac{1}{2}}). \quad (5.7)$$

Therefore we can redefine the scale (5.4) to have the form

$$\alpha = \bar{\alpha} \zeta (\log \zeta)^{\frac{1}{2}}, \quad (5.8)$$

where

$$\bar{\alpha} = 0(1).$$

To leading order, equation (5.2) reduces to

$$\hat{\phi}_0 = T_w - M_\infty^2 \hat{c}_0^2, \quad (5.9)$$

but in view of our comments above that $\hat{\phi}_0 \rightarrow 0$, as $\zeta \rightarrow \infty$, for $r = 0(1)$, then we have

$$\hat{c}_0 = \frac{T_w}{M_\infty}, \quad (5.10)$$

which means \hat{c}_0 is real.

At the first order in ϵ equation (5.2) has the form

$$\hat{\phi}_1 = T_1 + \frac{n^2 T_w}{\alpha^2 r^2} - M_\infty^2 (2 \hat{c}_0 \hat{c}_1 - 2 \hat{c}_0 \bar{w}_0), \quad (5.11)$$

while the $0(\epsilon)$ correction to the pressure equation (5.2) is given by

$$\frac{T_w}{\alpha^2} P_{rr} + \frac{T_w}{\alpha^2 r} P_r + \left[2 \hat{c}_0 M_\infty^2 (\hat{c}_1 - \bar{w}_0) - T_1 - \frac{n^2 T_w}{\alpha^2 r^2} \right] P = 0. \quad (5.12)$$

We now transform equation (5.12) using the same transformation as applied by Duck (12) for the basic flow. Firstly we employ the transform

$$\bar{r} = \ln r, \quad (5.13)$$

giving

$$\frac{T_w}{\alpha^2} e^{-2\bar{r}} P_{\bar{r}\bar{r}} + \left[2 \hat{c}_0 M_\infty^2 (\hat{c}_1 - \bar{w}_0) - T_1 - \frac{n^2 T_w}{\alpha^2} e^{-2\bar{r}} \right] P = 0. \quad (5.14)$$

Secondly we use the transform

$$\bar{R} = \int_0^{\bar{r}} \frac{d\bar{r}}{T_w}, \quad (5.15)$$

but since T_w is constant with respect to \bar{r} we can simplify (5.15) to

$$r = \bar{R} T_w. \quad (5.16)$$

where we take the constant of integration to be zero. Equation (5.14) can be re-written

$$P_{\bar{R}\bar{R}} + \left\{ \alpha^2 T_w [2 \hat{c}_0 M_\infty^2 (\hat{c}_1 - \bar{R}) - T_1] e^{2\bar{R} T_w} - n^2 T_w^2 \right\} P = 0, \quad (5.17)$$

where we have made use of the result obtained by Duck (12) for the basic flow

$$\bar{w}_0 = \bar{R}. \quad (5.18)$$

Equation (5.17) is solved numerically to obtain a value for \hat{c}_1 subject to the condition at the wall

$$P_{\bar{R}} \Big|_{\bar{R}=0} = 0, \quad (5.19)$$

and that P is bounded in the far-field. The second condition is obtained by taking $\bar{R} \rightarrow \infty$ limit of (5.17), i.e.

$$P_{\bar{R}\bar{R}} - \mu^2 \bar{R} e^{2\bar{R} T_w} P = 0, \quad (5.20)$$

$$\text{where} \quad \mu^2 = 2 \hat{c}_0 M_\infty^2 \alpha^2 T_w. \quad (5.21)$$

We find, to leading order, this equation has a decaying solution of the form

$$P \sim \mu^{-1/2} \bar{R}^{-1/4} \exp \left[-\frac{\mu}{T_w} e^{\bar{R} T_w} \bar{R}^{1/2} - \frac{1}{2} \bar{R} T_w \right]. \quad (5.22)$$

5.2 Numerical Results

All the results presented in this section correspond to a free-stream Mach number of 3.8, and azimuthal wavenumber $n=1$.

From our numerical observations we obtain a value for the leading order term in the c expansion (5.6) of the form

$$\hat{c}_0 \approx 0.4617922. \quad (5.23)$$

Using a fourth order Runge-Kutta scheme equation, (5.17) was solved subject to conditions (5.19) and (5.22) to determine the eigenvalues \hat{c}_1 . We find that for a given value of α there appears to be a large number of discrete, real values for \hat{c}_1 . Figure 5a displays a plot of \hat{c}_1 against α corresponding to the first five modes, as shown.

As observed above, our asymptotic analysis implies the existence of a large number of discrete possible values for \hat{c}_1 , which in turn implies the existence of a large number of discrete values for c_r . When we searched for the eigenvalues by solving the full system of equations numerically, for large ζ , we determined that there were indeed many modes and we managed to identify the first five modes. Figure 5b displays a comparison between the asymptotically determined value of c_r and the numerically determined value of c_r against ζ corresponding to the first mode. We have relatively good agreement, since the error term in the asymptotic theory is $O(\epsilon^2)$, which is quite large. Therefore the numerical results seem to confirm our asymptotic theory.

The asymptotic theory presented above tells us nothing about c_i and consequently reveals no information about the growth rate αc_i ; such an investigation would require a prohibitive amount of algebra.

We now move on to consider the form of the disturbance equations in the limit of small (large) ζ for cooled/heated wall conditions on a cone.

§6 Disturbance Equations for small ζ

In this section we consider the effect wall heating/cooling has on the asymptotic theory developed by DS for the limit $\zeta \rightarrow 0$ (and also with some simple modification the limit $\zeta \rightarrow \infty$ in the case of a cone) for the description of mode IA. It should be noted that the analysis in this section is also applicable for a cone, the circular cylinder case being retrieved when $\lambda = 0$. We find that when we impose heated/cooled wall conditions, instead of adiabatic conditions as treated by DS, the asymptotic theory is rather different. Here we consider the case of $\alpha \rightarrow 0$, $\zeta \rightarrow 0$. In DS it was shown that the disturbance equation for ϕ in the limit $\alpha \rightarrow 0$ (assuming $n \neq 0$) reduces to

$$\begin{aligned} \frac{d}{d\eta} \left\{ \frac{(w_0 - c)}{T_0} [1 + \lambda\zeta^2 + \zeta\eta] [(1 + \lambda\zeta^2 + \zeta\eta) \phi_\eta + \zeta\phi] - \frac{w_0\eta[1 + \lambda\zeta^2 + \zeta\eta]^2}{T_0} \phi \right\} \\ = \frac{n^2 \zeta^2}{T_0} \phi (w_0 - c). \end{aligned} \quad (6.1)$$

In the limit $\zeta \rightarrow 0$, we assume expansions for the $\eta = O(1)$ scale of the form

$$c = \zeta \bar{c}_1 + \zeta^2 \bar{c}_2 + \zeta^3 \bar{c}_3 + \dots, \quad (6.2)$$

$$\phi = \phi_0(\eta) + \zeta \phi_1(\eta) + \zeta^2 \phi_2(\eta) + \zeta^3 \phi_3(\eta) + \dots, \quad (6.3)$$

$$w_0 = w_{00}(\eta) + \zeta w_{01}(\eta) + \zeta^2 w_{02}(\eta) + \zeta^3 w_{03}(\eta) + \dots, \quad (6.4)$$

$$T_0 = T_{00}(\eta) + \zeta T_{01}(\eta) + \zeta^2 T_{02}(\eta) + \zeta^3 T_{03}(\eta) + \dots, \quad (6.5)$$

where $w_{00}(\eta)$ and $T_{00}(\eta)$ represent the planar values of the velocity and temperature profiles respectively, and $w_{01}(\eta)$ and $T_{01}(\eta)$ etc. correspond to the perturbations to the basic flow caused through curvature. A more complete expansion for ϕ is given in DS.

To leading order, we have for $\eta = O(1)$ that

$$\phi_0 = A_0 w_{00}(\eta), \quad (6.6)$$

where A_0 represents an arbitrary amplitude parameter.

At the next order in ζ we obtain the equation for φ_1

$$\begin{aligned} w_{00} \varphi_{1\eta} - A_0 w_{00\eta} \bar{c}_1 + A_0 w_{00}^2 - w_{00\eta} \varphi_1 \\ + A_0 w_{01} w_{00\eta} - A_0 w_{01\eta} w_{00} = k_1 T_{00} , \end{aligned} \quad (6.7)$$

where we have used equation (6.6) and k_1 is a constant. Setting $\eta = 0$ in equation (6.7) and assuming $\varphi_1|_{\eta=0} = 0$ we have

$$- A_0 \bar{c}_1 w_{00\eta} (\eta=0) = k_1 T_{00} (\eta=0). \quad (6.8)$$

The boundary conditions as $\eta \rightarrow \infty$, must be compatible with the form of system (6.1) in the far-field (as presented in DS), together with (6.6).

Defining

$$\bar{r} = 1 + \eta \zeta = O(1), \quad (6.9)$$

then we must have an outer solution of the form

$$\varphi_0^{\text{out}} = \hat{A} \bar{r}^{-n-1}, \quad (6.10)$$

where

$$\hat{A} = A_0 + \zeta \hat{A}_1 + \dots, \quad (6.11)$$

and so we must also have

$$\varphi_{1\eta}|_{\eta \rightarrow \infty} = \varphi_0^{\text{out}} \Big|_{\bar{r}=1} = -(n+1)A_0. \quad (6.12)$$

Substituting this into (6.7) yields

$$\bar{c}_1 = \frac{n T_{00} (\eta=0)}{w_{00\eta} (\eta=0)}. \quad (6.13)$$

In order to obtain complex values of c in our asymptotic analysis we must consider higher orders in ζ .

At the next order of ζ we have the system

$$\begin{aligned}
 & w_{00} \varphi_{2\eta} + 2\lambda w_{00} \varphi_{0\eta} + 2\eta w_{00} \varphi_{1\eta} + w_{02} \varphi_{0\eta} \\
 & - w_{02\eta} \varphi_0 + w_{01} \varphi_{1\eta} + \eta^2 w_{00} \varphi_{0\eta} - \bar{c}_1 \varphi_{1\eta} \\
 & + 2 w_{01} \eta \varphi_{0\eta} + w_{01} \varphi_0 - w_{01\eta} \varphi_1 - 2\eta w_{01\eta} \varphi_0 \\
 & - 2\eta \bar{c}_1 \varphi_{0\eta} - \bar{c}_2 \varphi_{0\eta} + w_{00} \varphi_1 + \eta w_{00} \varphi_0 \\
 & - \bar{c}_1 \varphi_0 - w_{00\eta} \varphi_2 - 2\lambda w_{00\eta} \varphi_0 - 2\eta \varphi_1 w_{00\eta} \\
 & - \eta^2 w_{00\eta} \varphi_0 = k_2 T_{00} + \eta^2 T_{00} \int_0^\eta \frac{\varphi_0 w_{00}}{T_{00}} d\eta \\
 & + k_1 T_{01}.
 \end{aligned} \tag{6.14}$$

We now determine the leading order imaginary component of the complex wavespeed c . Since (6.14) contains only real coefficients, any imaginaries must, of necessity, only arise at a critical point, where $c = w_{00}$. Since $c = O(\zeta)$, this must occur when $\eta = O(\zeta)$. We therefore consider a thin layer relative to the $\eta = O(1)$ scale, namely

$$\bar{y} = \eta/\zeta = O(1). \tag{6.15}$$

On this scale, the expansion for φ is expected to develop as

$$\varphi = \zeta \bar{\varphi}_0(\bar{y}) + \zeta^2 \bar{\varphi}_1(\bar{y}) + \zeta^3 \bar{\varphi}_2(\bar{y}) + \dots, \tag{6.16}$$

where the $\bar{\varphi}_i$ are expected to be normalised in such a way as to be generally $O(1)$ quantities.

The leading order equation has the form

$$\bar{\varphi}_0 = A_0 \bar{y} w_{00\eta}(\eta=0) \tag{6.17}$$

(where A_0 was introduced in equation (6.6)).

At the next order in ζ we obtain the system

$$\begin{aligned}
 & [w_{00\eta}(0) \bar{y} - \bar{c}_1] \bar{\varphi}_{1\bar{y}} - \bar{\varphi}_1 w_{00\eta}(0) = \bar{k}_1 \\
 & + \frac{1}{2} \bar{y}^2 w_{00\eta\eta}(0) A_0 w_{00\eta}(0) - \frac{A_0 \bar{c}_1 w_{00\eta}(0)}{T_{00}(0)} T_{00\eta}(0) \bar{y},
 \end{aligned} \tag{6.18}$$

where \bar{k}_1 is a constant term. This system cannot be simplified any further, as in DS, since the condition $w_{00\eta\eta}(\eta=0) = 0$, no longer holds

in the present (i.e. heated/cooled wall) case.

As in DS, we assume A_0 and \bar{k}_1 to be real quantities, as we are at liberty to do so, and now consider Φ_1^i (where i denotes an imaginary component). This quantity is triggered by the $+i\pi$ jump in the logarithm across the critical layer. We can re-write (6.18) in the form

$$[w_{00\eta}(0) \bar{y} - \bar{c}_1] \Phi_{1\bar{y}} - \Phi_1 w_{00\eta}(0) = \hat{R}, \quad (6.19)$$

where

$$\hat{R} = \bar{k}_1 + \frac{1}{2} \bar{y}^2 w_{00\eta\eta}(0) A_0 w_{00\eta}(0) - \frac{A_0 \bar{c}_1 w_{00\eta}(0)}{T_{00}(0)} T_{00\eta}(0) \bar{y}, \quad (6.20)$$

and find

$$\Phi_1 = [w_{00\eta}(0) \bar{y} - \bar{c}_1] \int_0^{\bar{y}} \frac{\hat{R} d\bar{y}}{[w_{00\eta}(0) \bar{y} - \bar{c}_1]^2}. \quad (6.21)$$

Evaluating this integral, taking just the imaginaries together with the limit as $\bar{y} \rightarrow \infty$ yields

$$\begin{aligned} \Phi_1^i &\sim \pi A_0 \bar{c}_1 [w_{00\eta}(0) \bar{y} - \bar{c}_1] \left\{ \frac{w_{00\eta\eta}(0)}{w_{00}^2 \eta(0)} - \frac{T_{00\eta}(0)}{T_{00}(0) w_{00\eta}(0)} \right\} \\ &= B^i [w_{00\eta}(0) \bar{y} - \bar{c}_1], \end{aligned} \quad (6.22)$$

$$\text{where } B^i = \pi A_0 \bar{c}_1 \left\{ \frac{w_{00\eta\eta}(0)}{w_{00}^2 \eta(0)} - \frac{T_{00\eta}(0)}{T_{00}(0) w_{00\eta}(0)} \right\}. \quad (6.23)$$

Equation (6.22) now provides a lower boundary condition for systems (6.7) and (6.14).

Assuming (6.7) contains real coefficients only (\bar{c}_1 is assumed real, an assumption that may be justified a posteriori) we have

$$\Phi_1^i = B^i w_{00}(\eta), \quad (6.24)$$

where B^i is defined in (6.23).

Considering the imaginary part of system (6.14) in the limit $\eta \rightarrow \infty$ we obtain

$$\varphi_{2\eta}^i \Big|_{\eta \rightarrow \infty} + \varphi_1^i \Big|_{\eta \rightarrow \infty} = k_2^i. \quad (6.25)$$

By the form of φ in the far-field (as presented in DS) we require

$$\begin{aligned} \varphi_{2\eta}^i \Big|_{\eta \rightarrow \infty} &\sim - (n+1) \varphi_1^i \Big|_{\eta \rightarrow \infty} \\ &\sim - (n+1) B^i, \end{aligned} \quad (6.26)$$

and therefore

$$k_2^i = - B^i n. \quad (6.27)$$

We now consider the imaginary part of (6.14) evaluated at $\eta = 0$

$$- \bar{c}_1 \varphi_{1\eta}^i \Big|_{\eta=0} - \bar{c}_2^i \varphi_{0\eta} \Big|_{\eta=0} - w_{00\eta}(0) \varphi_2^i \Big|_{\eta=0} = k_2^i T_{00}(0). \quad (6.28)$$

Using the results

$$\begin{aligned} \varphi_{1\eta}^i \Big|_{\eta=0} &= B^i w_{00\eta}(0), \\ \varphi_2^i \Big|_{\eta=0} &= - B^i \bar{c}_1, \end{aligned} \quad (6.29)$$

we obtain

$$\bar{c}_2^i = n^2 \frac{\pi T_{00}^2(\eta=0)}{w_{00}^3(\eta=0)} \left\{ \frac{w_{00\eta\eta}(\eta=0)}{w_{00\eta}(\eta=0)} - \frac{T_{00\eta}(\eta=0)}{T_{00}(\eta=0)} \right\}. \quad (6.30)$$

Using the governing equations of motion we can simplify (6.30) to the form

$$\bar{c}_2^i = n^2 \frac{2\pi T_{00}^2(0) w_{00\eta\eta}(0)}{4 w_{00\eta}^2(0)}. \quad (6.31)$$

Comparing this result with the adiabatic result, as obtained in DS, we note that the first imaginary term in c is an order in ζ larger for heated/cooled wall conditions, implying larger growth rates in the present case. The ratio of the leading-order imaginary terms has the form

$$\frac{\text{Heated/Cooled } c_i}{\text{Adiabatic } c_i} = \frac{2 w_{00} \eta(0)}{\zeta w_{00} \eta(0) [1 + 2\sigma M_\infty^2 (\gamma - 1)n]} . \quad (6.32)$$

We find, however, that altering the wall conditions from adiabatic conditions as treated by DS, to heated/cooled wall conditions, has little significant effect on the asymptotic analysis for the mode I lower neutral point for which $\alpha = O(\zeta^{\frac{1}{2}})$.

§7. Conclusions

In this paper we have investigated the supersonic boundary-layer flow, and the inviscid stability thereof, over axisymmetric bodies (with particular emphasis on a long thin, straight circular cylinder) subject to heated or cooled wall conditions.

The effect of wall cooling is, generally, seen to reduce the importance of the "first mode" of inviscid instability, while the amplification rates of the "second mode" of inviscid instability are increased. Therefore we have agreement with the effect wall cooling has on planar boundary layers (Mack (11), for example).

The converse effect is observed with wall heating. The amplification rates of the "first mode" of instability increases, while wall-heating causes the "second mode" of instability to be stabilized. Wall-heating may also cause the formation of a second subsonic generalised inflexional mode, which results in the appearance of an additional mode of instability, not found in adiabatic or cooled-wall studies.

Asymptotic studies for large azimuthal wavenumbers and far downstream distances reveal that the real part of the eigenvalue c is non-unique in both limits, suggesting that there exists an infinite number of discrete possible values for the real part of c in both these limits, although the corresponding values of the imaginary part of c are exceedingly small.

Acknowledgements

This research was supported by the National Aeronautics and Space Administration under NASA contract No. NAS1 - 18605 while one of the authors (PWD) was in residence at the Institute for Computer Applications in Science and Engineering (ICASE), NASA Langley Research Centre, Hampton, VA 23665. S.J.S. was in the receipt of a Northern Ireland Education Department Studentship. A number of computations were carried out with computer time provided under S.E.R.C. Grant No. GR/E/25702, and by the University of Manchester.

References

1. Lees, L and Lin, C.C. Investigation of the stability of the laminar boundary layer in a compressible fluid, NACA Tech. Note No. 1115, (1946).
2. Mack, L.M. Boundary-layer linear stability theory in "Special course on stability and transition of laminar flow", AGARD Report No. 709, 3-1, (1984).
3. Lees, L. The stability of the laminar boundary layer in a compressible fluid, NACA Tech. Report No. 876, (1947).
4. Van Driest, E.R. Calculation of the stability of the laminar boundary layer in a compressible fluid on a flat plate with heat transfer. J. Aero. Sci. 19, 801-12, (1952).
5. Dunn, D.W. and Lin, C.C. On the stability of the laminar boundary layer in a compressible fluid, J. Aero. Sci., Vol. 22, pp. 455-477. (1955).
6. Mack, L.M. The inviscid stability of the compressible laminar boundary layer, in "Space programs summary", no. 37-23, p.297. JPL, Pasadena CA, (1963).
7. Mack, L.M. The inviscid stability of the compressible laminar boundary layer: Part II, in "Space programs summary", No. 37-26, Vol. IV p165, JPL Pasadena, CA, (1964).
8. Mack, L.M. Stability of the compressible laminar boundary layer according to a direct numerical solution, in AGARDograph 97, part I, 329, (1965).

9. Mack, L.M. Computation of the stability of the laminar boundary layer, in "Methods in computational physics". (B. Alder, S. Fernbach and M. Rotenberg eds). Vol 4, 247, Academic, N.Y., (1965).
10. Mack, L.M. Boundary-layer stability theory, JPL, Pasadena, CA, Document No. 900-277, Rev A, (1969).
11. Mack, L.M. Review of compressible stability theory in Proc. ICASE workshop on the stability of time dependent and spatially varying flows, Springer-Verlag, (1987).
12. Duck, P.W. The inviscid axisymmetric stability of the supersonic flow along a circular cylinder. ICASE Report No. 89-19, (1989), [also J. Fluid Mech. 214, 611 1990].
13. Duck, P.W. and Shaw, S.J. The inviscid stability of supersonic flow past a sharp cone. ICASE Report No. 90-14, (1990). To appear in Theo. and Comp. Fluid Dyn.
14. Seban, R.A. and Bond, R. Skin friction and heat transfer characteristics of a laminar boundary layer on a cylinder in axial incompressible flow. J. Aero. Sci. 10, 671, (1951).
15. Duck, P.W. and Bodonyi, R.J. The wall jet on an axisymmetric body. Quart. J. Mech. Appl. Maths. 39, 407, (1986).
16. Abramowitz, M. and Stegun, I.A. Handbook of Mathematical functions. Dover Publications, Inc., New York, (1965).

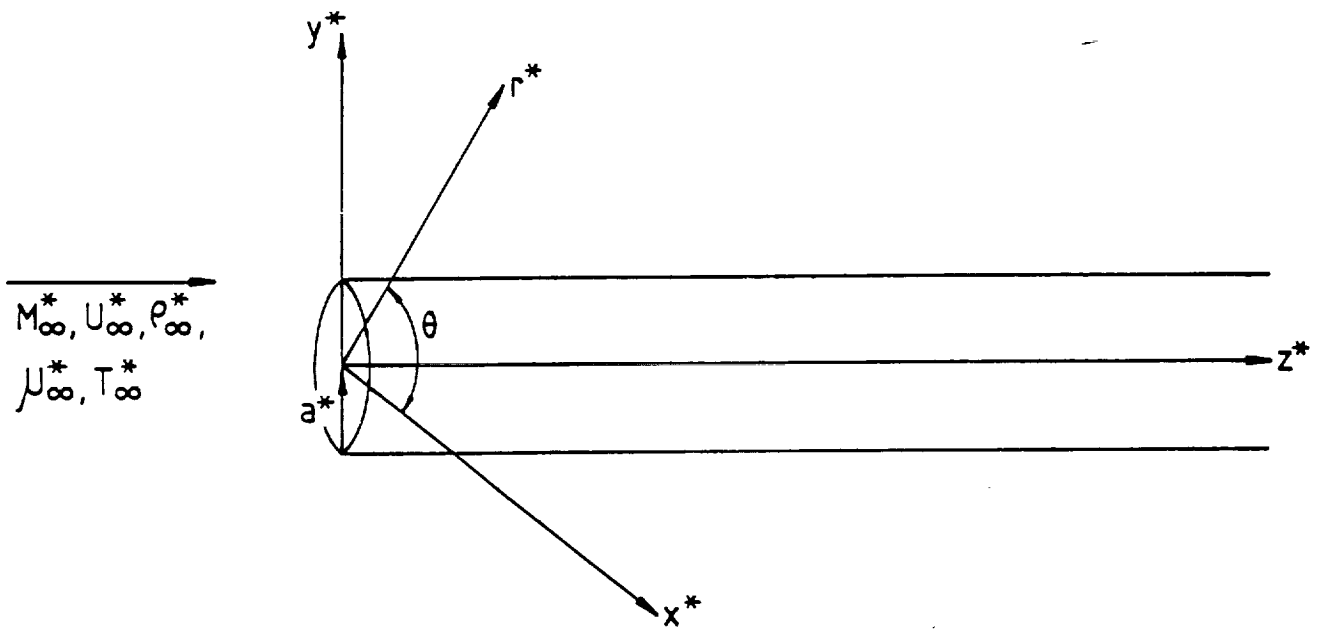


Fig 1 Layout

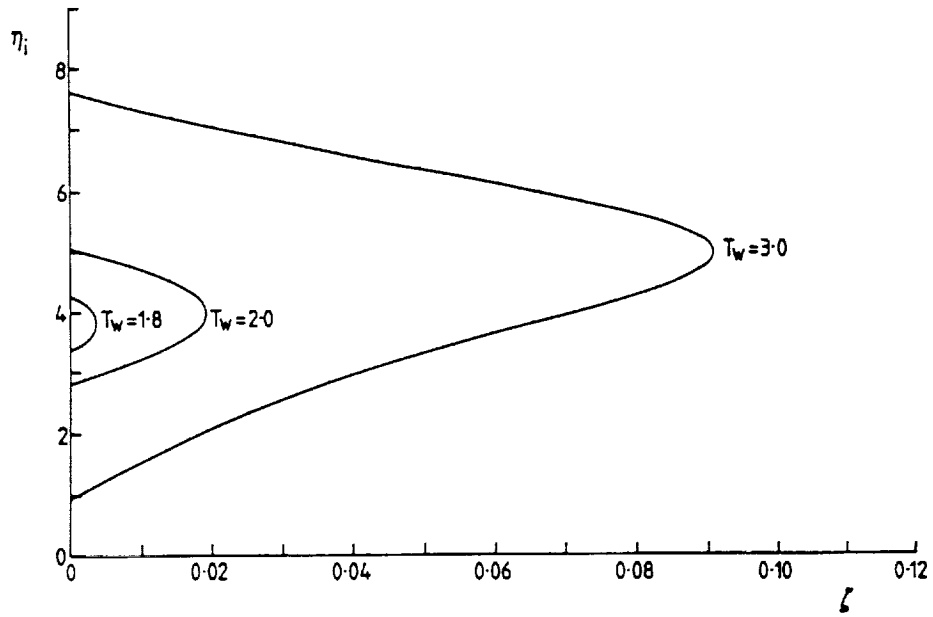


Fig 2a Variation of transverse positions of inflexion points (η_i) with axial locations (ζ), $M_\infty = 3.8$.

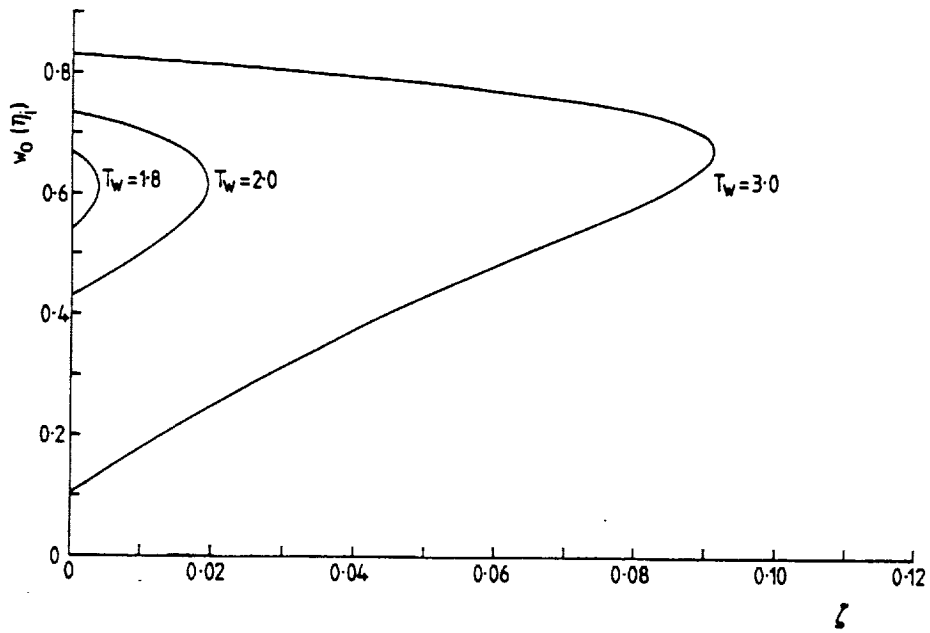


Fig 2b Variation of $w_0(\eta=\eta_i)$ with ζ , $M_\infty = 3.8$.

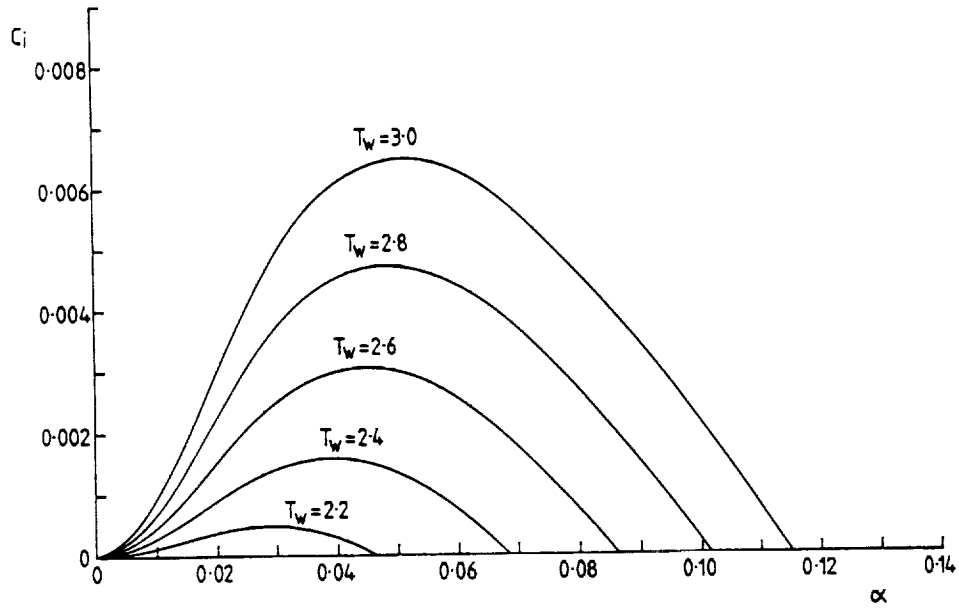


Fig 2c Variation of c_i with α , $M_\infty=3.8$, $\zeta=0$, Mode I (Planar).

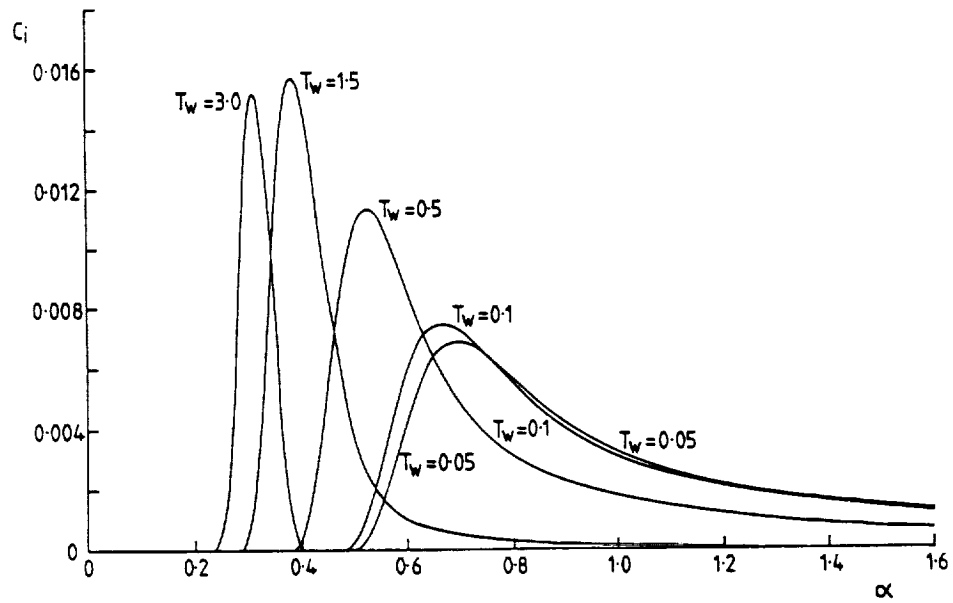


Fig 2d Variation of c_i with α , $M_\infty=3.8$, $\zeta=0$, Mode II (Planar).

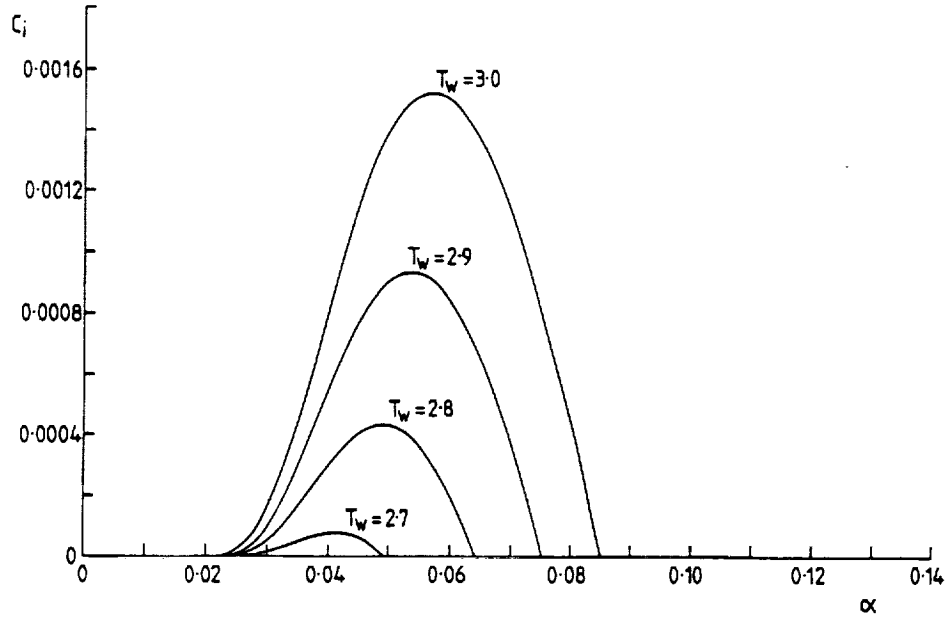


Fig 2e Variation of c_i with α , $M_\infty=3.8$, $\zeta=0.05$, $n=0$, Mode I.

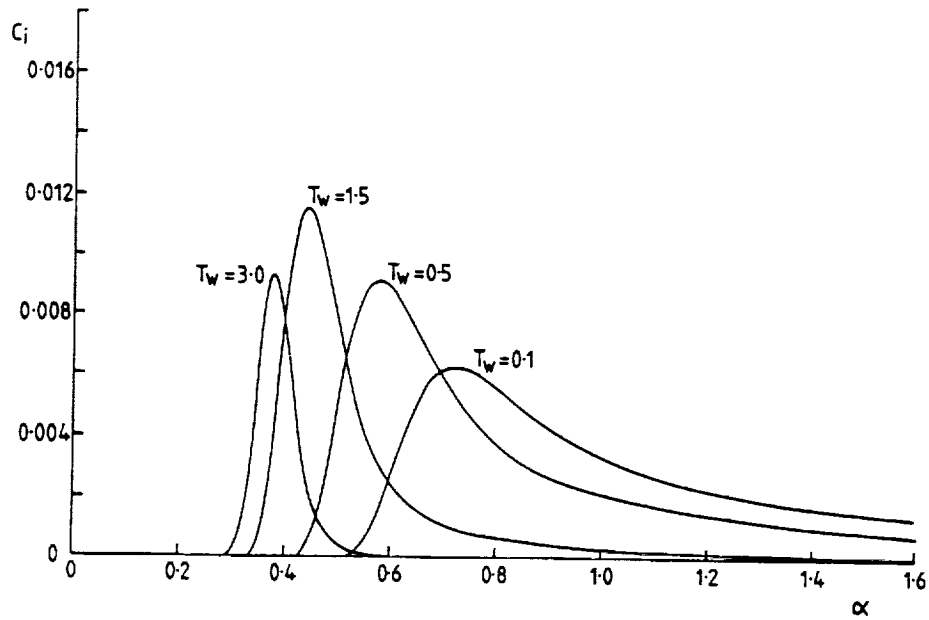


Fig 2f Variation of c_i with α , $M_\infty=3.8$, $\zeta=0.05$, $n=0$, Mode II.

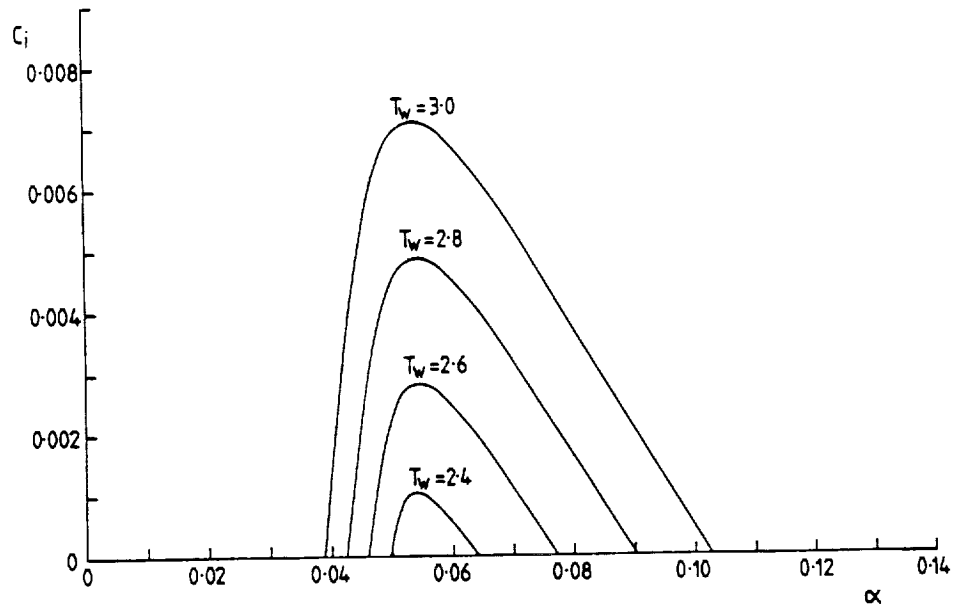


Fig 2g Variation of c_i with α , $M_\infty=3.8$, $\zeta=0.05$, $n=1$, Mode I.

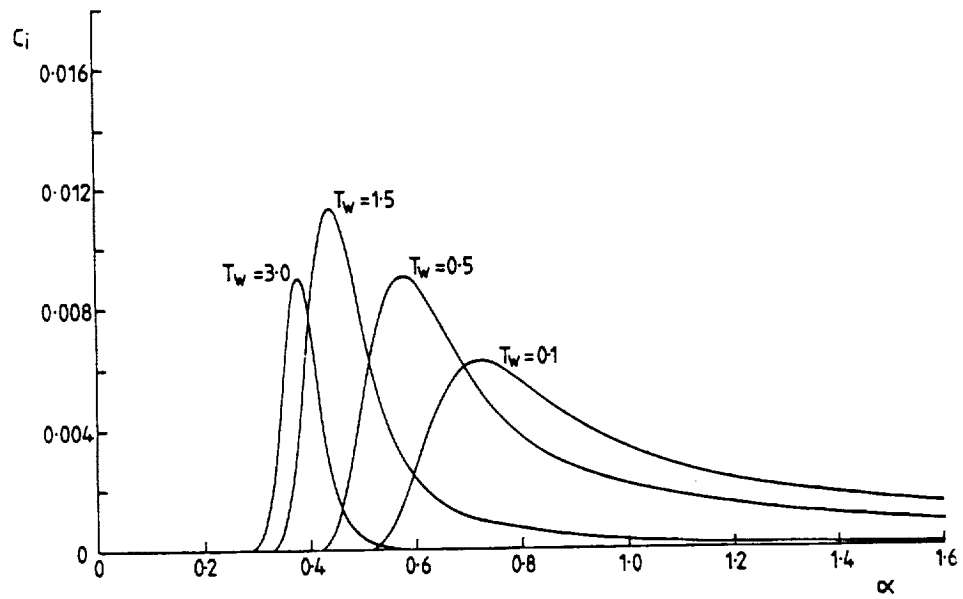


Fig 2h Variation of c_i with α , $M_\infty=3.8$, $\zeta=0.05$, $n=1$, Mode II.

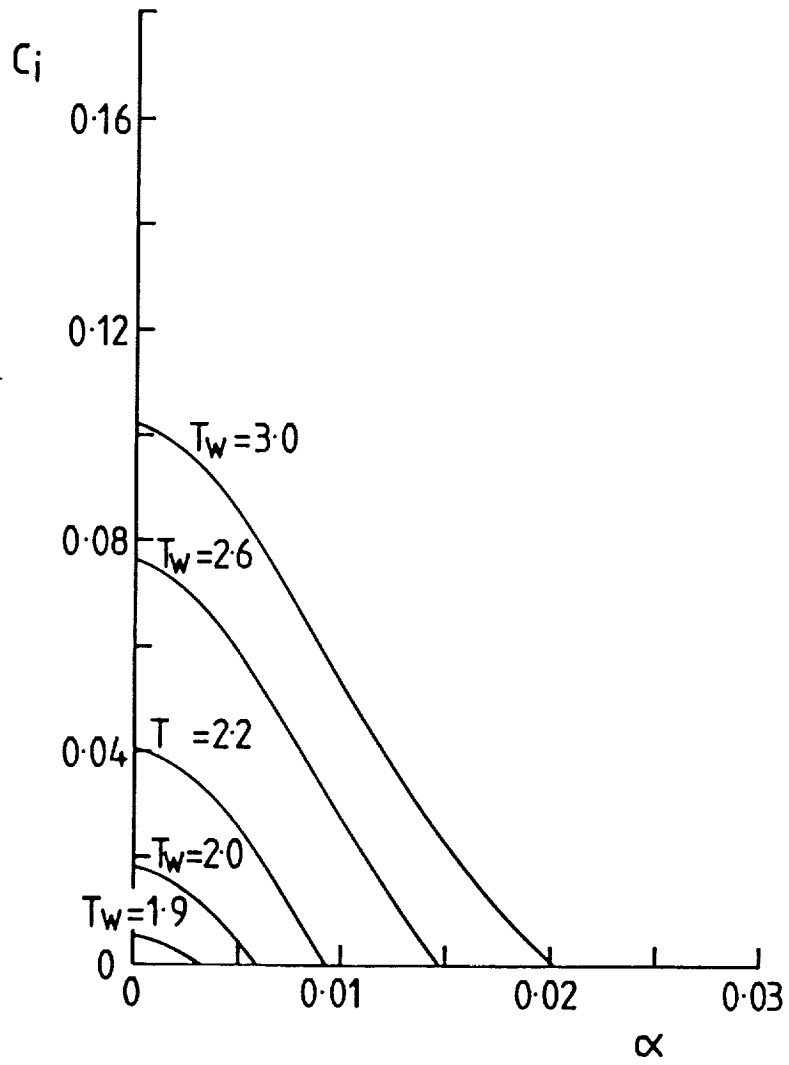


Fig 2i Variation of c_i with α , $M_\infty=3.8$, $\zeta=0.05$, $n=1$, Mode IA.

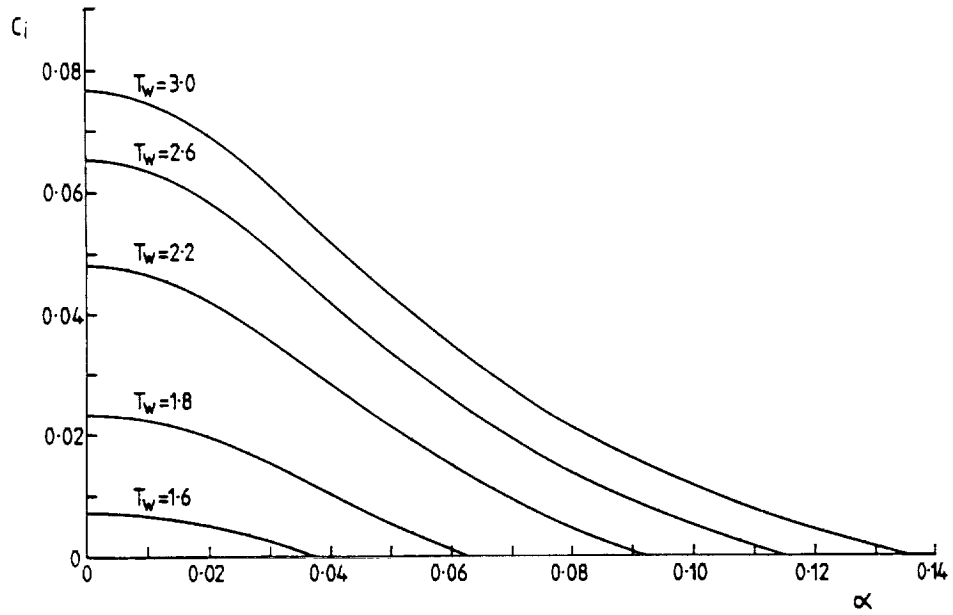


Fig 2j Variation of c_i with α , $M_\infty=3.8$, $\zeta=0.05$, $n=3$, Mode I.

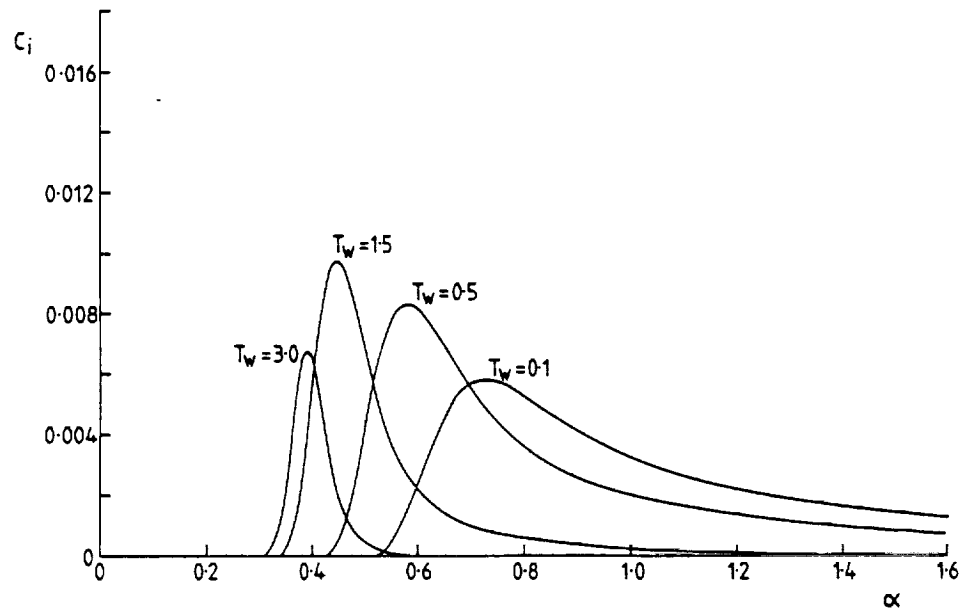


Fig 2k Variation of c_i with α , $M_\infty=3.8$, $\zeta=0.05$, $n=3$, Mode II.

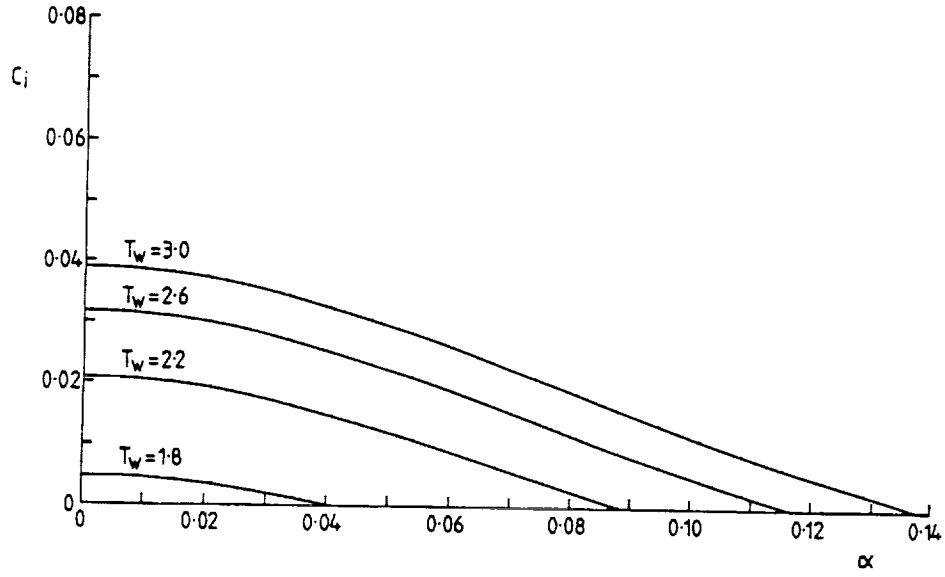


Fig 2l Variation of c_i with α , $M_\infty=3.8$, $\zeta=0.05$, $n=5$, Mode I.

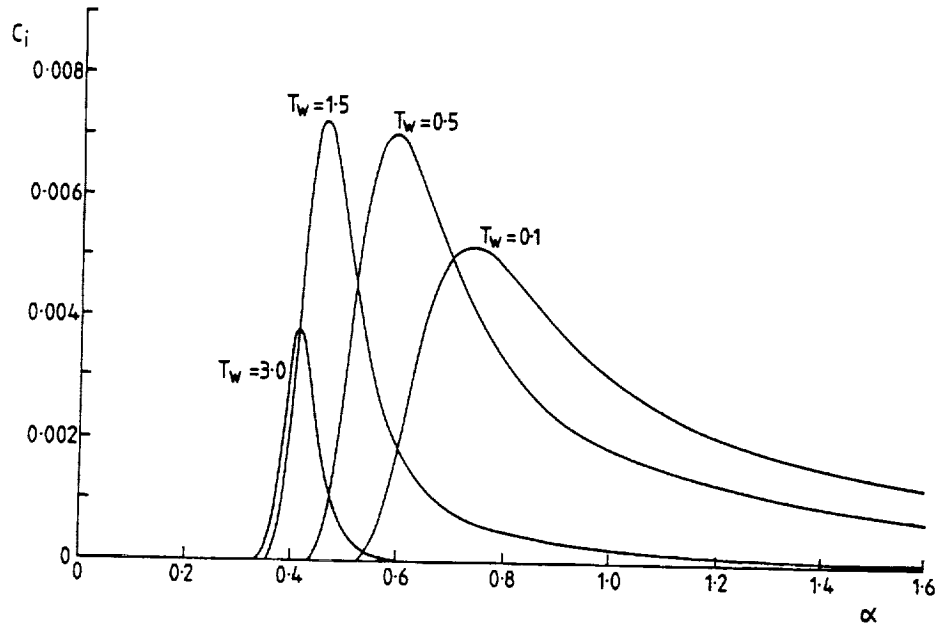


Fig 2m Variation of c_i with α , $M_\infty=3.8$, $\zeta=0.05$, $n=5$, Mode II.

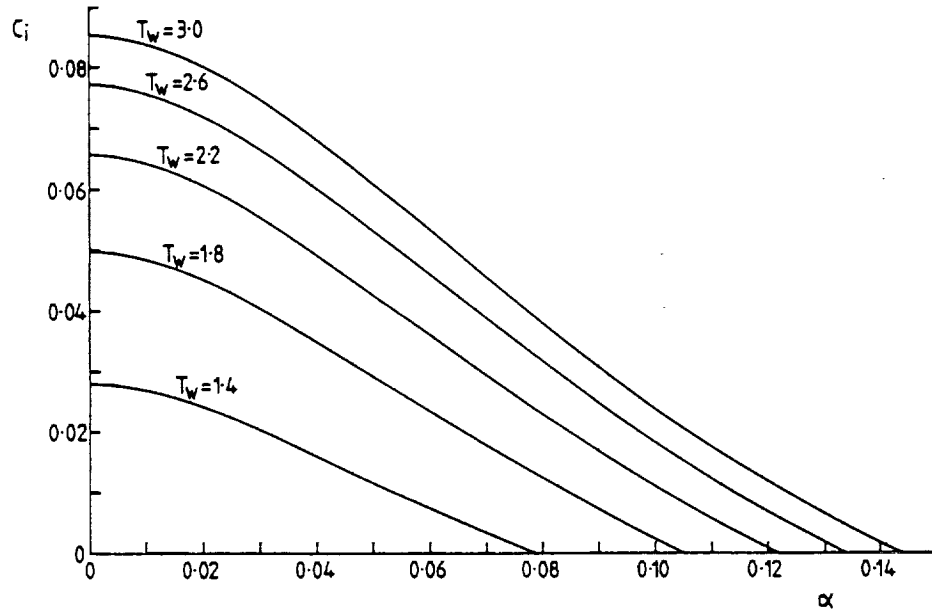


Fig 2n Variation of c_i with α , $M_\infty=3.8$, $\zeta=0.5$, $n=1$, Mode I.

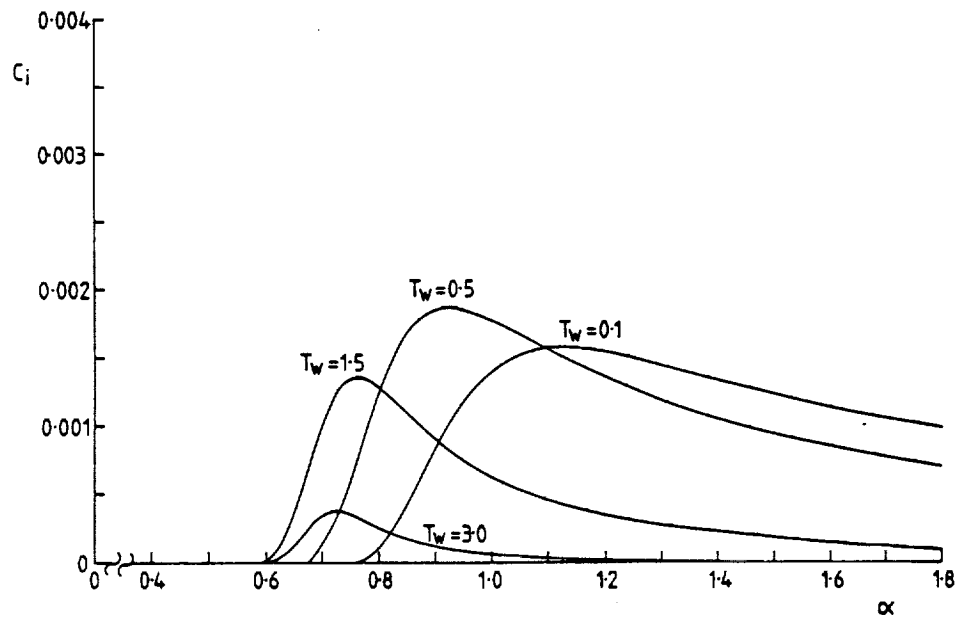


Fig 2o Variation of c_i with α , $M_\infty=3.8$, $\zeta=0.5$, $n=1$, Mode II.

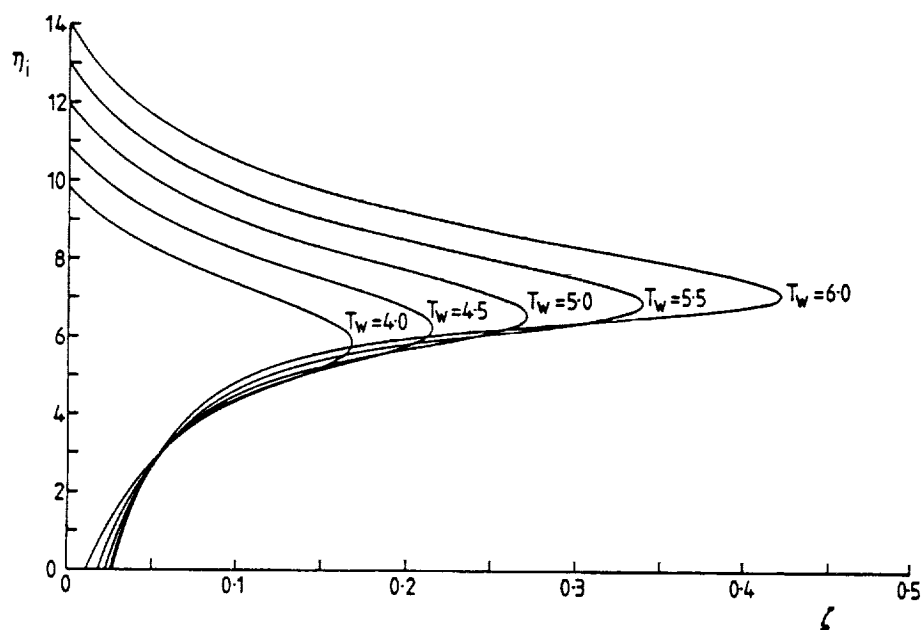


Fig 3a Variation of transverse positions of inflexion points (η_i) with axial locations (ζ), $M_\infty=3.8$.

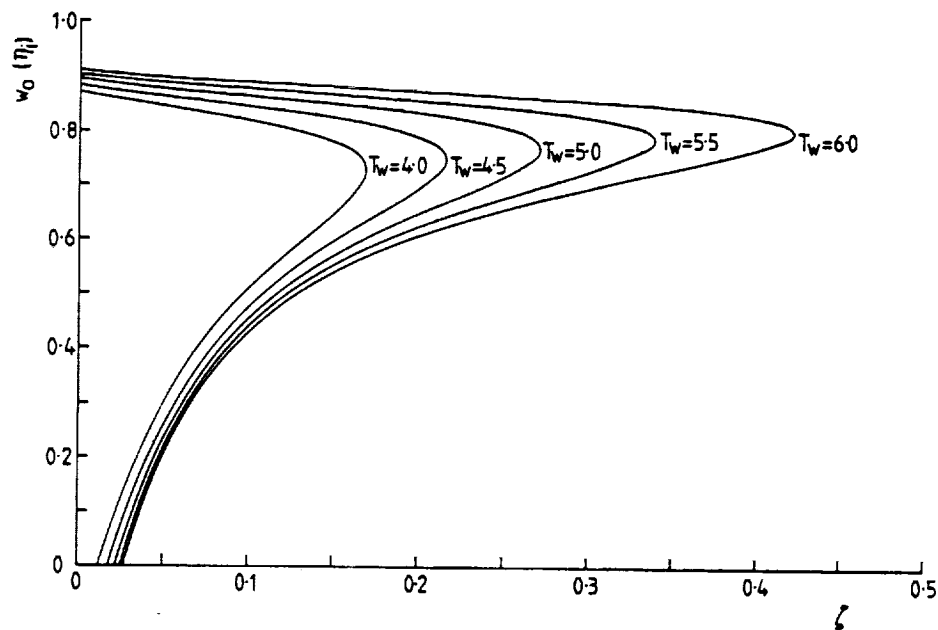


Fig 3b Variation of $w_0(\eta=\eta_i)$ with ζ , $M_\infty=3.8$.

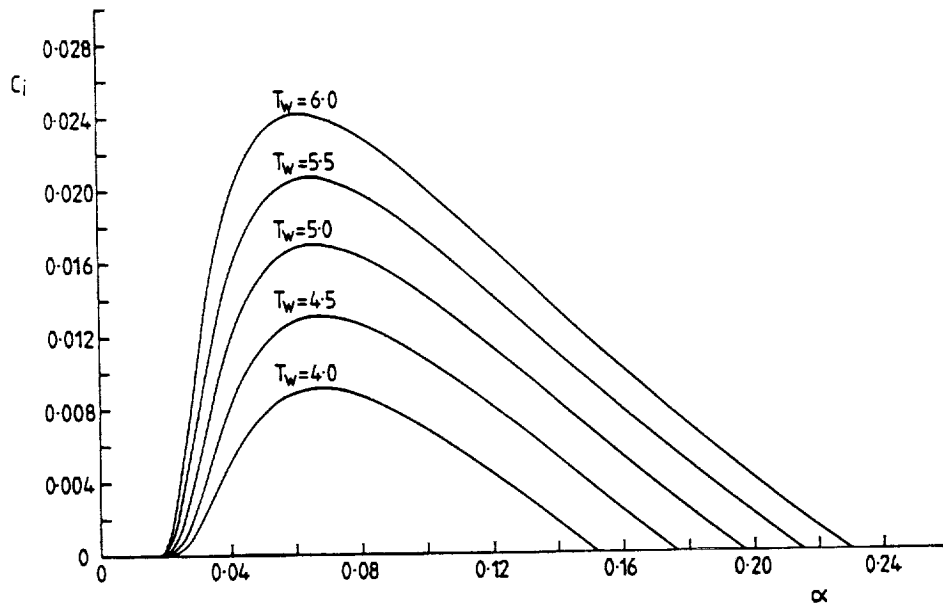


Fig 3c Variation of c_i with α , $M_\infty=3.8$, $\zeta=0.05$, $n=0$, Mode I.

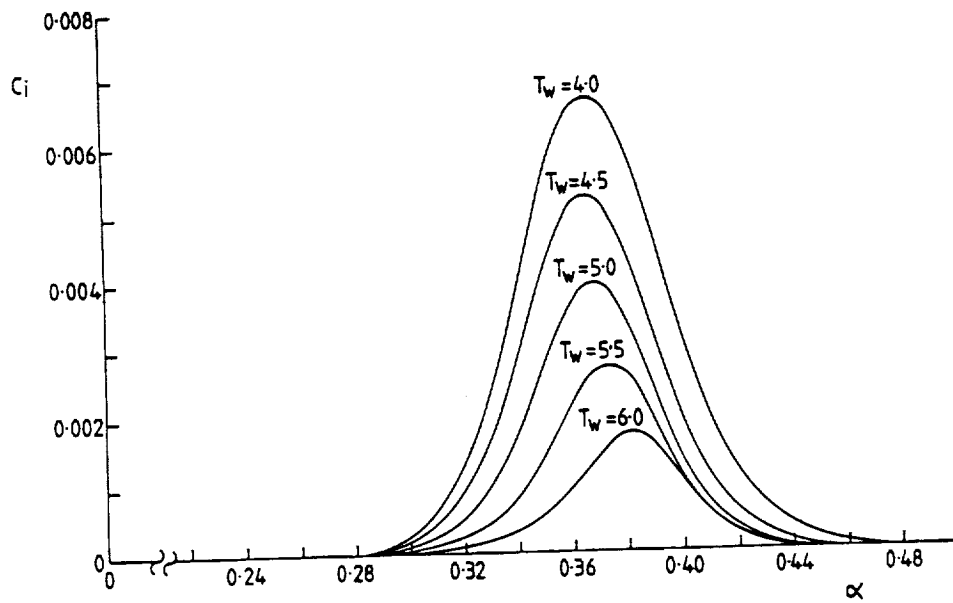


Fig 3d Variation of c_i with α , $M_\infty=3.8$, $\zeta=0.05$, $n=0$, Mode II.

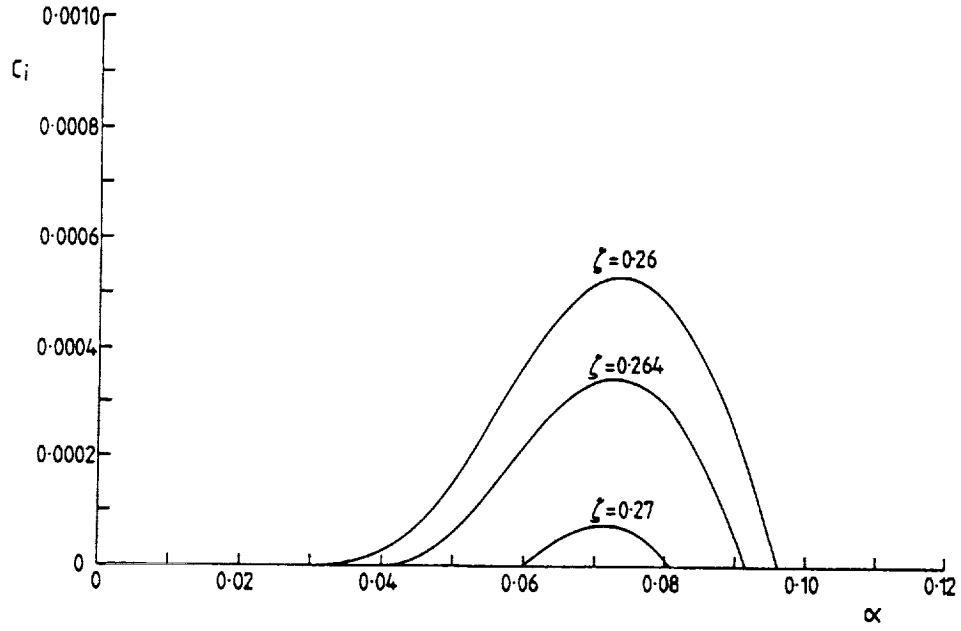


Fig 3e Variation of c_i with α , $M_\infty=3.8$, $T_w=5.0$, $n=0$, Mode I.

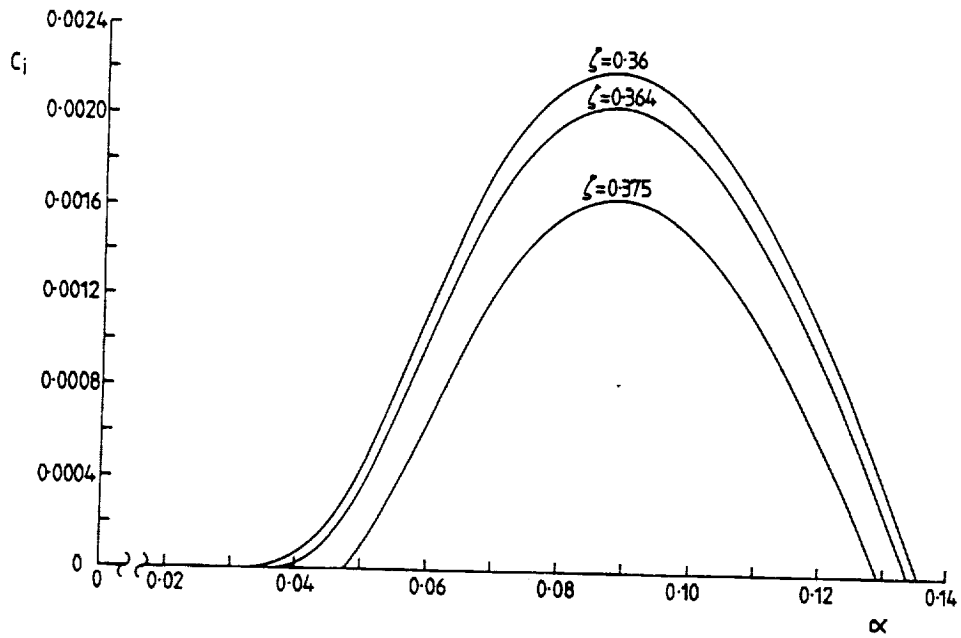


Fig 3f Variation of c_i with α , $M_\infty=3.8$, $T_w=6.0$, $n=0$, Mode I.

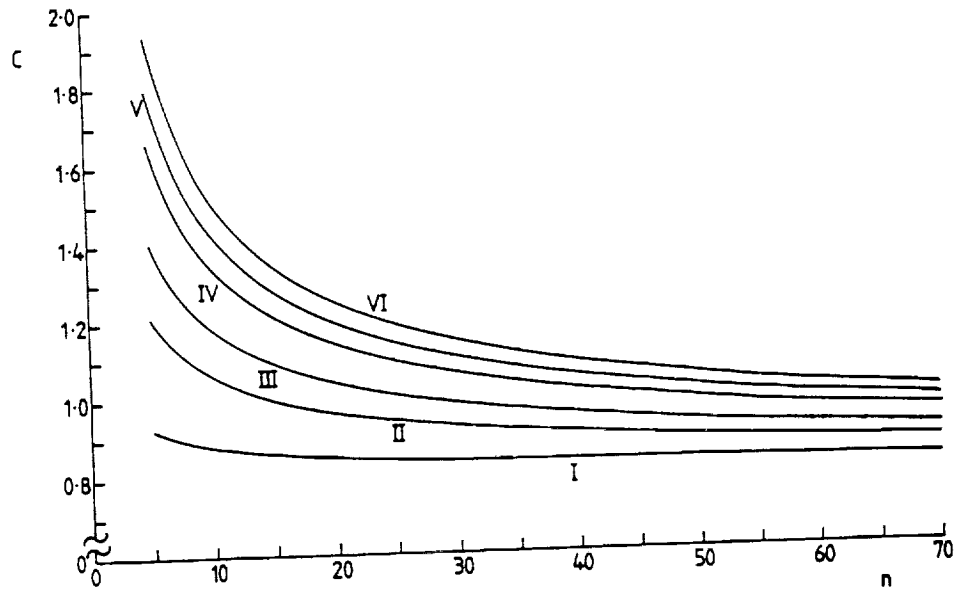


Fig 4a Variation of the asymptotically determined value of c with n .

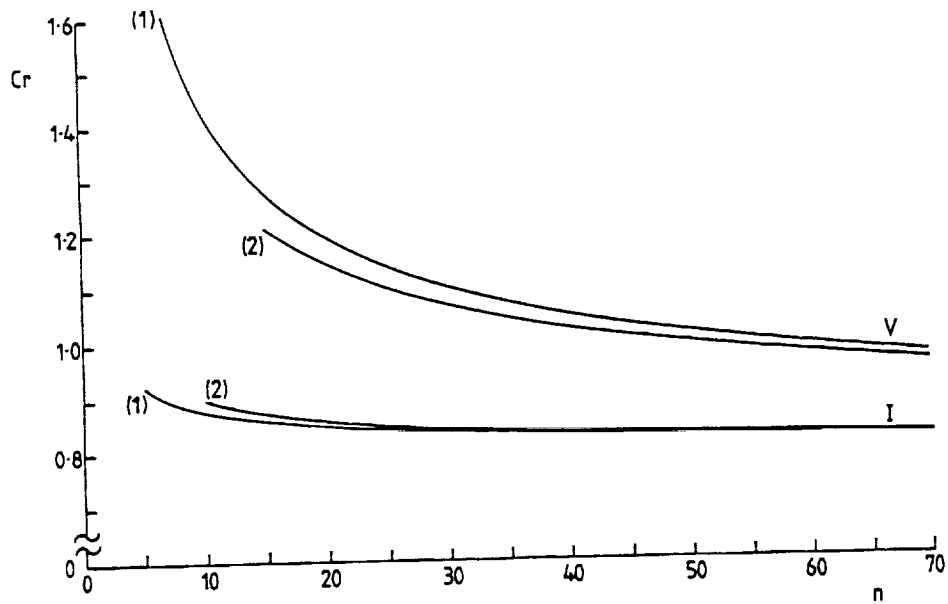


Fig 4b Comparison of computed c_r with asymptotic form.

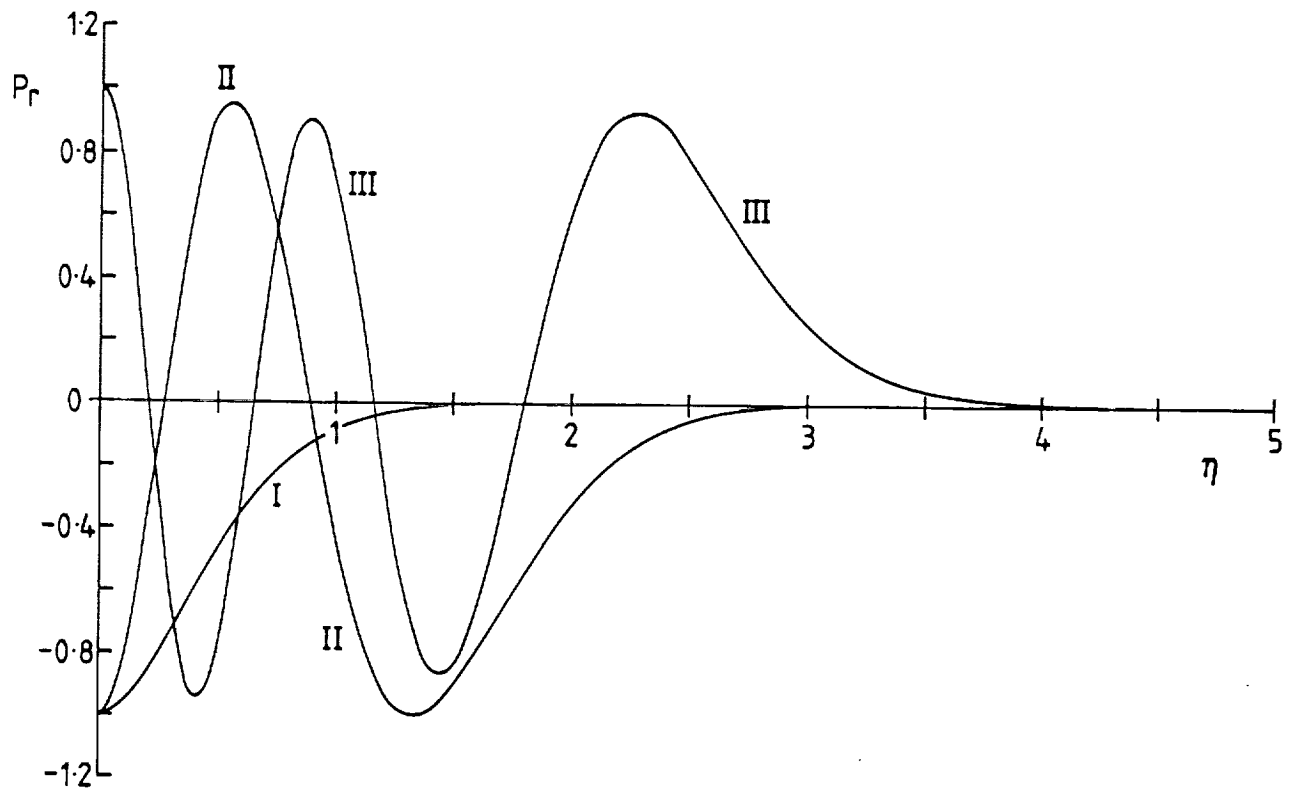


Fig 4c Variation of $P_r = \text{Real}\{P\}$ with η .

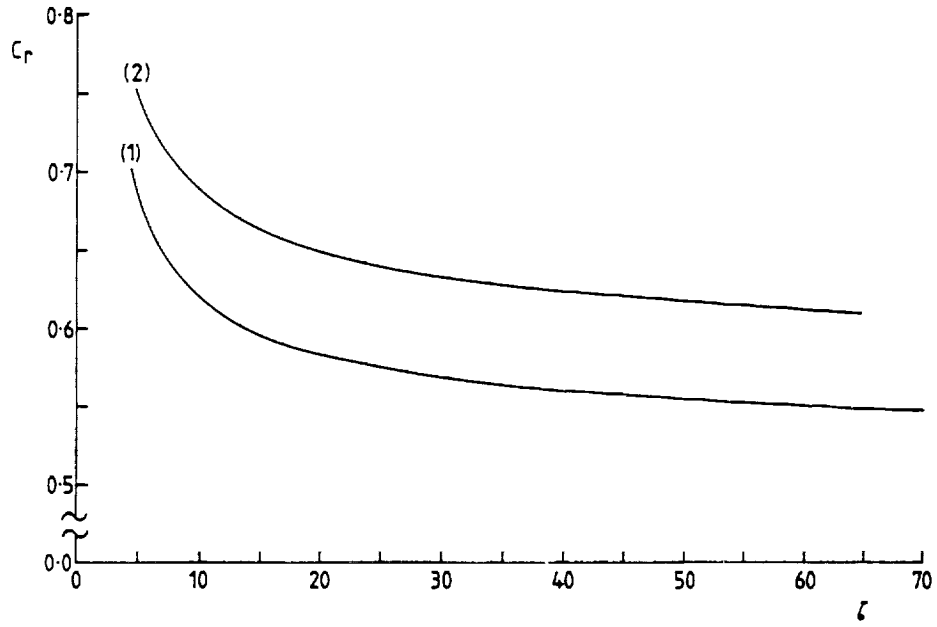


Fig 5b Comparison of computed c_r with asymptotic form.

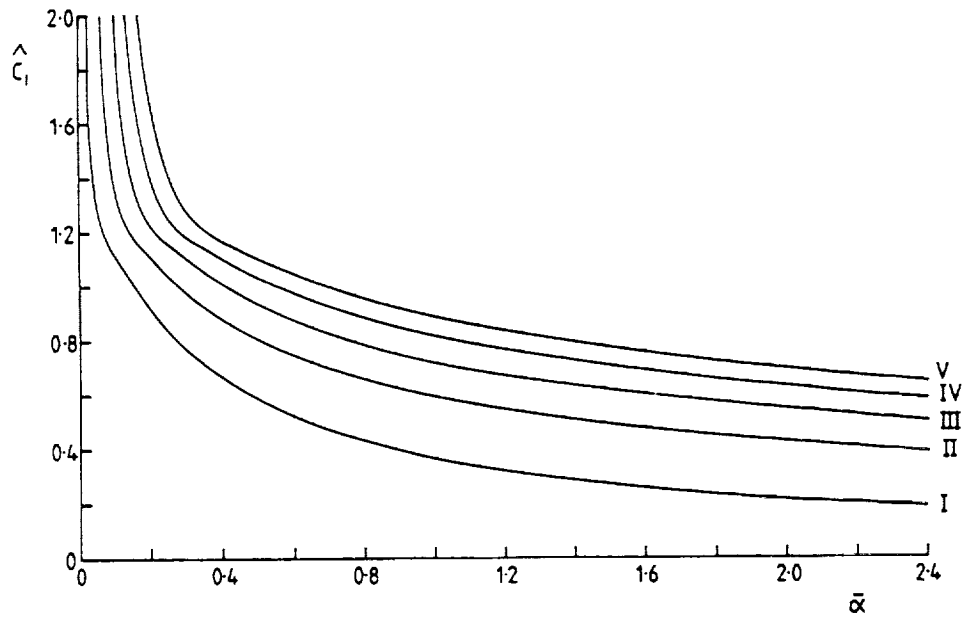


Fig 5a Variation of \hat{c}_1 with $\bar{\alpha}$.

1. Report No. NASA CR-187475 ICASE Report No. 90-81		2. Government Accession No.		3. Recipient's Catalog No.	
4. Title and Subtitle THE INVISCID STABILITY OF SUPERSONIC FLOW PAST HEATED OR COOLED AXISYMMETRIC BODIES				5. Report Date November 1990	
				6. Performing Organization Code	
7. Author(s) Stephen J. Shaw Peter W. Duck				8. Performing Organization Report No. 90-81	
				10. Work Unit No. 505-90-21-01	
9. Performing Organization Name and Address Institute for Computer Applications in Science and Engineering Mail Stop 132C, NASA Langley Research Center Hampton, VA 23665-5225				11. Contract or Grant No. NAS1-18605	
				13. Type of Report and Period Covered Contractor Report	
12. Sponsoring Agency Name and Address National Aeronautics and Space Administration Langley Research Center Hampton, VA 23665-5225				14. Sponsoring Agency Code	
15. Supplementary Notes Langley Technical Monitor: Richard W. Barnwell Submitted to Physics of Fluids Final Report					
16. Abstract The inviscid, linear, non-axisymmetric, temporal stability of the boundary layer associated with the supersonic flow past axisymmetric bodies (with particular emphasis on long thin, straight circular cylinders), subject to heated or cooled wall conditions is investigated. The eigenvalue problem is computed in some detail for a particular Mach number of 3.8, revealing that the effect of curvature and the choice of wall conditions both have a significant effect on the stability of the flow. Both the asymptotic, large azimuthal wavenumber solution and the asymptotic, far downstream solution are obtained for the stability analysis and compared with numerical results. Additionally, asymptotic analyses valid for large radii of curvature with cooled/heated wall conditions, are presented. We find, in general, important differences exist between the wall temperature conditions imposed in this paper and the adiabatic wall conditions considered previously. NASA FORM 10					
17. Key Words (Suggested by Author(s)) inviscid stability, supersonic flow, axisymmetric body			18. Distribution Statement 02 - Aerodynamics Unclassified - Unlimited		
19. Security Classif. (of this report) Unclassified	20. Security Classif. (of this page) Unclassified		21. No. of pages 53	22. Price A04	

